NASA TECHNICAL NOTE

NASA TN D-4136

NASA TN D-4136

BOILING HEAT-TRANSFER COEFFICIENTS, INTERFACE BEHAVIOR, AND VAPOR QUALITY IN ROTATING BOILER OPERATING TO 475 G'S

by

Vernon H. Gray and Paul J. Marto

Lewis Research Center
Cleveland, Ohio

and

Allan W. Joslyn

Manned Spacecraft Center
Houston, Texas

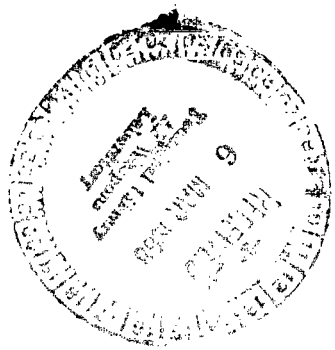

NATIONAL AERONAUTICS AND SPACE ADMINISTRATION • WASHINGTON, D. C. • MARCH 1968

NASA TN D-4136

BOILING HEAT-TRANSFER COEFFICIENTS, INTERFACE BEHAVIOR, AND VAPOR QUALITY IN ROTATING BOILER OPERATING TO 475 G'S

By Vernon H. Gray and Paul J. Marto

Lewis Research Center
Cleveland, Ohio

and

Allan W. Joslyn

Manned Spacecraft Center
Houston, Texas

NATIONAL AERONAUTICS AND SPACE ADMINISTRATION

For sale by the Clearinghouse for Federal Scientific and Technical Information
Springfield, Virginia 22151 – CFSTI price $3.00

BOILING HEAT-TRANSFER COEFFICIENTS, INTERFACE BEHAVIOR, AND VAPOR QUALITY IN ROTATING BOILER OPERATING TO 475 G'S

by Vernon H. Gray, Paul J. Marto, and Allan W. Joslyn

Lewis Research Center

SUMMARY

An experimental heated-wall rotating boiler was investigated with continuous through-flow of water as the test fluid. Heat-transfer coefficients were obtained with the boiler stationary and at rotative accelerations to 200 g's. Heat fluxes up to 505 000 Btu per hour per square foot (1.59 MW/m^2) were employed in obtaining the coefficients. Photographic and boiler-performance data were obtained to 475 g's. Outlet vapor quality, measured by throttling calorimeters, varied from above 99 percent to several degrees of vapor superheat.

High-speed motion pictures revealed that high accelerations nearly eliminated disturbances at the liquid-vapor interface, reduced the number and size of bubbles, and promoted direct evaporation across the interface by the mechanism of convective secondary-flow cells in the rotating fluid annulus.

Boiling heat-transfer coefficients at low heat fluxes were increased by increases in acceleration. At high heat fluxes the opposite was true, although the variation in coefficient was small and comparable with that caused by surface conditioning and aging effects. The crossover points for the coefficients occurred at progressively higher heat-flux levels as acceleration was increased. A boiling heat-transfer coefficient as high as 9000 Btu per hour per square foot per ^{o}F (51.2 $kW/(m^2)(^{o}K)$) was measured (at the highest heat-flux value). Boiler-test performance was quite satisfactory and warranted consideration of the rotating boiler concept in Rankine cycle systems for power generation.

INTRODUCTION

Boilers and vapor-generation devices are being reevaluated and extensively revised because of new requirements imposed on them by spaceflight applications and by the use of nuclear reactors as heat sources. Such boilers are required to operate at high heat-

flux levels and under low-, variable-, and zero-gravity fields. They also must be reliable and stable during extended operation. These requirements necessitate a forced-flow type of "once-through" boiler, which differs greatly from a conventional, recirculating boiler that uses earth gravity for separation of the vapor from the liquid.

Several techniques for achieving the preceding boiler requirements are currently under study at the NASA Lewis Research Center. One of these techniques is to rotate the boiler and utilize high centrifugal accelerations to forcibly separate the vapor from the liquid phase. A feasibility study of this concept was made (ref. 1), which presents the advantages and disadvantages, and a scheme for its application to a Rankine cycle system.

Published experimental data on the effects of high rotative accelerations on nucleate boiling are limited. Pool-boiling heat-transfer coefficients were reported at accelerations to 21 g's by Merte and Clark in reference 2; to 40 g's by Costello and Tuthill in reference 3; to 9 g's by Graham and Hendricks in reference 4; and limited data to 100 g's by Beckman and Merte in reference 5. Peak nucleate boiling, or burnout, heat fluxes to 45 g's were measured by Costello and Adams (ref. 6), and to 157 g's by Ivey (ref. 7). In these experiments, a pool of liquid was rotated with a small, isolated heating element (such as a tube or ribbon) immersed in it.

This investigation was conducted to obtain nucleate-boiling heat-transfer data for water at higher gravity levels than those previously reported, to evaluate the performance of a rotating boiler with continuous through-flow of fluid, to measure exit vapor quality, and to determine the effect of acceleration on interface disturbances.

In this study, a 4-inch (10.2-cm) inside-diameter, electrically heated, cylindrical boiler concentric with the vertical axis of rotation, was operated over the following range of variables:

Rotative acceleration, earth gravities	None to 475
Heat flux, Btu/(hr)(ft^2); kW/m^2	12 400 to 505 000; 39.2 to 1590
Inlet liquid subcooling, ^oF; ^oK	3 to 141; 1.7 to 78
Inlet liquid flow rate, lb/hr; kg/hr	0 to 86.4; 0 to 39.2
Exit vapor pressure	Atmospheric

A motion-picture film supplement that shows the effects of rotation on boiling and liquid-vapor separation has been prepared and is available on loan. A request card and a description of this film are included at the back of the report.

EXPERIMENTAL APPARATUS

The test apparatus is shown schematically in figure 1, and the general layout of the equipment is presented in figure 2.

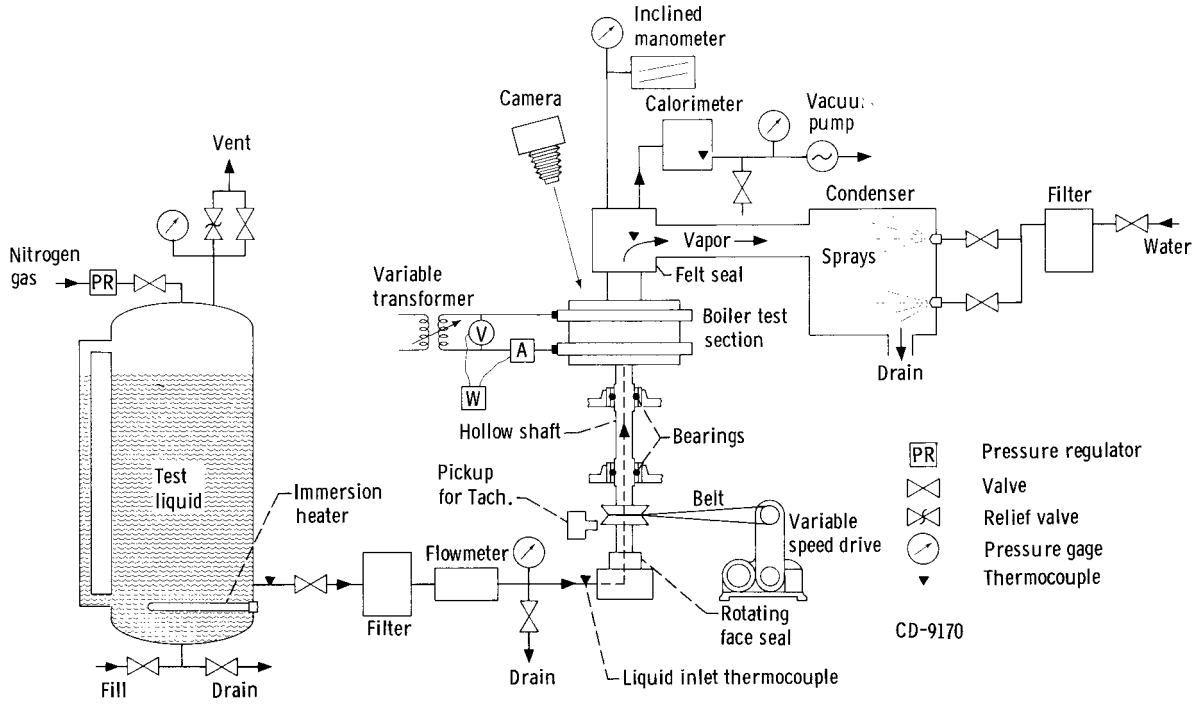

Figure 1. - Schematic diagram of test apparatus for rotating boiler.

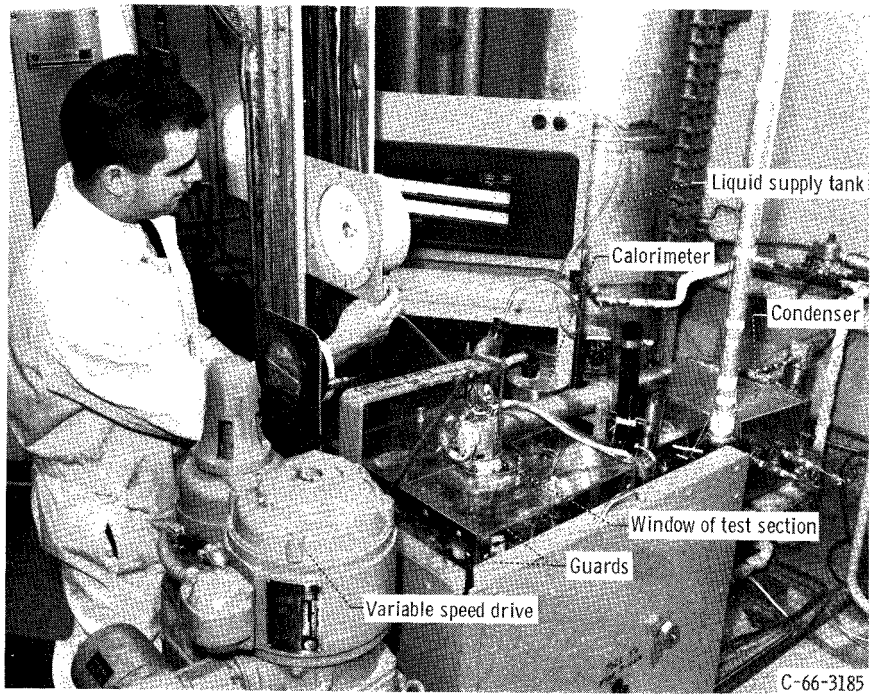

Figure 2. - Overall view of rotating boiler test installation.

Liquid Supply System

Demineralized triple-distilled water was used in the experiments. This water was stored in the large stainless-steel supply tank shown in figure 1. The tank had two immersion-type heaters used to degas the liquid and preheat it to about 200° F (367° K).

The distilled water was pressure fed through a porous metal filter and a microflow turbine-type flowmeter. Nitrogen gas at about 30 psig (207 kN/m^2 gage) was used to pressurize the tank. The feed lines were stainless steel tubes with a 3/8-inch (0.95-cm) outside diameter. The tubes were trace heated with 1/4-inch (0.63-cm) copper steam lines and wrapped with asbestos strips. The feed liquid passed through a graphite-to-stone rotating face seal and into the hollow shaft.

Boiler-Condenser

The test boiler was a 4-inch- (10.2-cm-) inside-diameter copper cylinder, 2 inches high (5.1 cm). It was designed to rotate at speeds up to 3000 rpm. The boiler was mounted on top of a vertical shaft driven by a pulley and V-belt from a variable-speed drive.

A detailed cross-sectional drawing of the boiler test section is shown in figure 3. Liquid flowed upward inside the vertical shaft, passed through a regulating valve, and then sprayed out to the cylindrical walls where it formed a liquid annulus. New liquid passed up into the heated zone through eight small holes (0.078-in. or 0.198-cm diam) to replace the fluid that boiled off. Vapor produced in the boiling process separated from the fluid annulus (because of centrifugal force) and flowed out the top of the boiler along the axis of rotation.

The thickness of the fluid annulus was maintained nearly constant over a wide range of heating rates and rotative speeds by a float-activated linkage to the needle valve. As the fluid layer thickness built up, the free surface became a paraboloid (nearly cylindrical at higher rotative speeds). The buoyant force tended to push the float inward closing off the orifice of the regulating valve. As the fluid boiled away, the float moved outward opening the orifice and allowing more water into the boiler. During most of the runs, the water thickness was set for about 1/4 to 3/8 inch (0.63 to 0.95 cm) by the adjustment screw shown in figure 3. An enlarged view of the float and needle valve linkage is presented in figure 4.

Heat flowed radially into the boiler from an 11-gage Chromel-A heater wire in a 3/16-inch (0.47-cm-) outside diameter Inconel sheath with alumina insulation. This heater was helically wound and furnace-brazed into a helical recess machined in the outside surface of the cylindrical copper boiler wall. Fiberglass insulation was packed

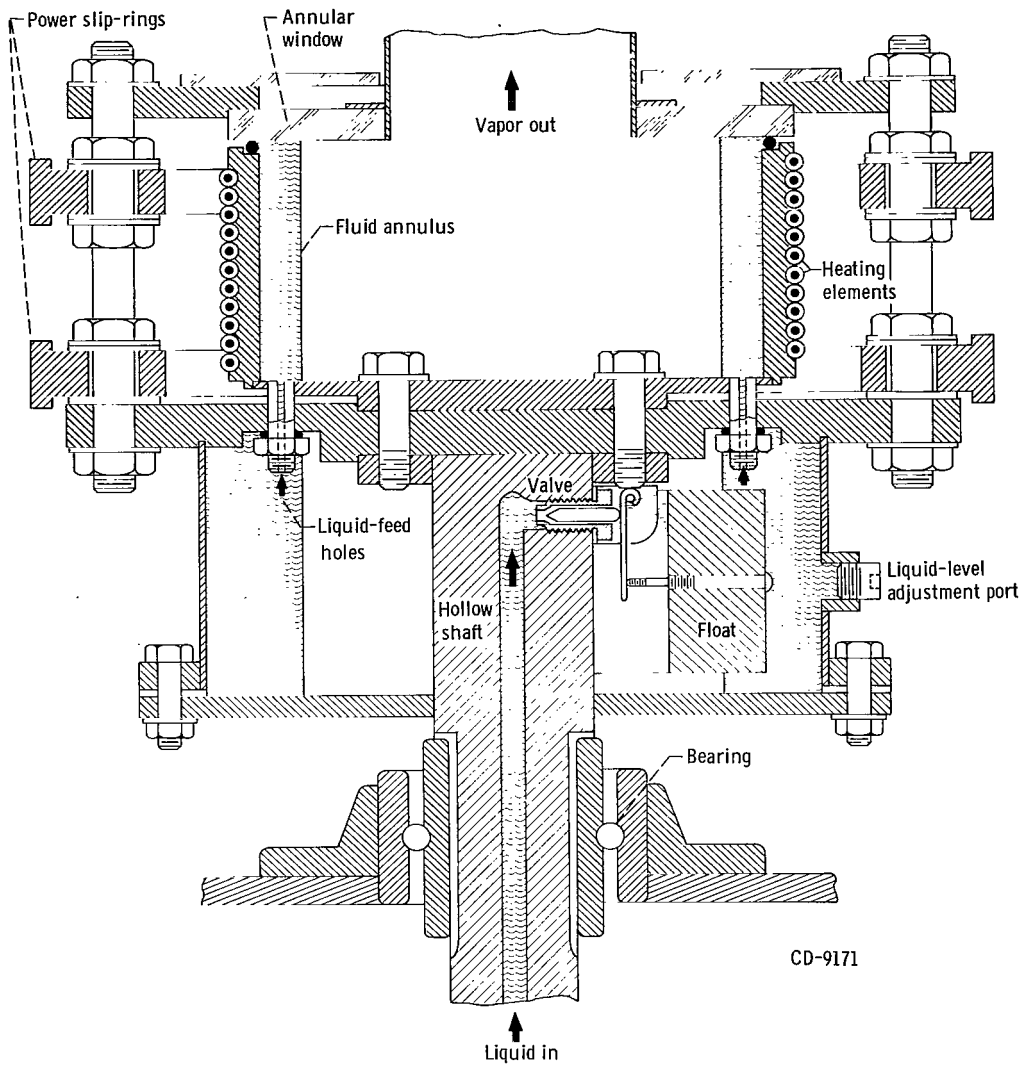

Figure 3. - Cross-section of rotating boiler test section.

around the float chamber and heater coils to reduce heat losses. The copper heat-transfer surface of the boiler was hot wiped with a layer of pure tin about 5 mils (0.13 mm) thick.

Clear preshrunk plastic windows were installed in the annular region on top of the boiler so that the liquid-vapor interface and the boiling action could be photographed. An enlarged view of the boiler assembly with the top window and outlet duct removed is presented in figure 5. The slip rings and brushes for the electrical power supply (multiple variable transformers) are also shown in the figure.

The outlet vapor duct engaged a stationary felt rubbing seal in the 2-inch- (5.1-cm-) diameter pipe assembly leading to the condenser. The condenser was a cubical metal

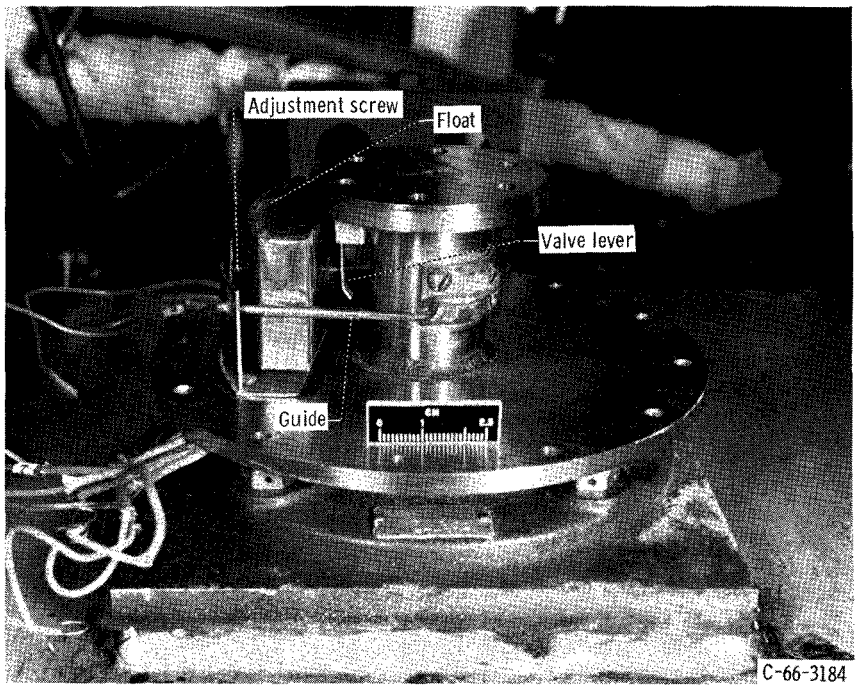

Figure 4. - Rotating float valve assembly.

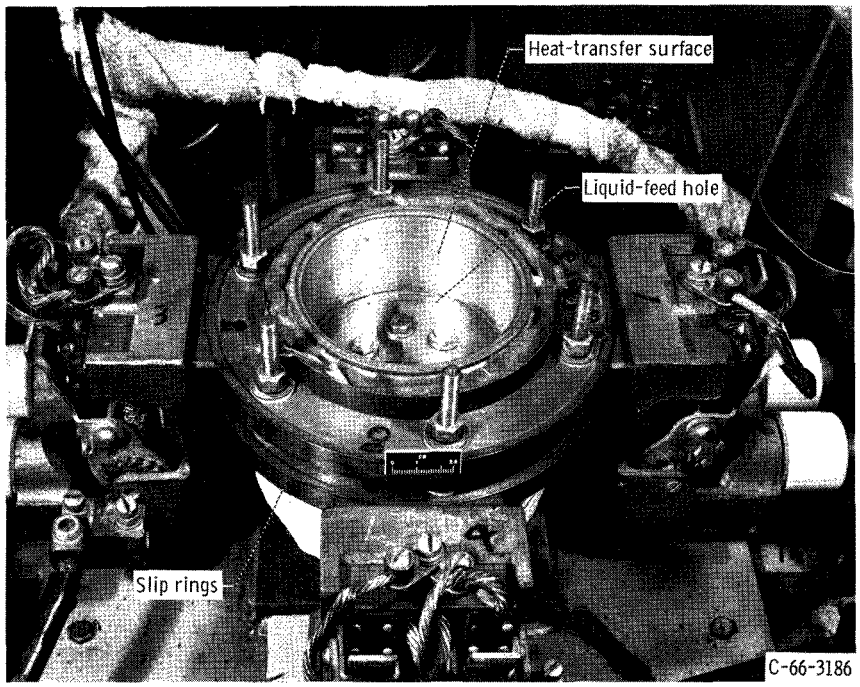

Figure 5. - View of boiler showing heat-transfer surface and power slip rings.

box open to the atmosphere at the bottom. Four nozzles, two on either side of the vapor inlet, sprayed cold tap water into the condenser box. The condensate and spray water drained out at the bottom of the box.

Photographic System

As shown in figure 1, cameras were mounted above the boiler to look vertically downward at the liquid-vapor interface. Several cameras were used: a 4- by 5-inch (10.2- by 12.7-cm) bellows type with a 270-millimeter lens and a 1-microsecond flash; a 16-millimeter high-speed motion-picture camera capable of 8000 frames per second (70-mm lens); and a 16-millimeter motion-picture camera capable of 26 000 frames per second. Color and black-and-white film were used with backlighting reflected from the bottom of the boiler.

Instrumentation

The boiling test instrumentation is shown schematically in figure 1, and the test section thermocouple details are shown in figure 6. Two thermocouples rotated with the boiler; their leads were brought out of the system through four silver slip rings, each with two silver-graphite brushes. The heated-boiler-wall rotating thermocouple was a single 26-gage constantan wire joined to the copper wall with solder at the end of a drilled hole 0.040 inch (0.102 cm) in diameter, 1 inch (2.54 cm) up from the bottom of the heated cylinder, 0.098±0.002 inch (0.25±0.005 cm) from the cylinder inside diameter. The second rotating thermocouple measured the temperature of the local boiling fluid at a point 1/8 inch (0.32 cm) radially inward from the heated wall surface and 1 inch (2.54 cm) up from the bottom. This thermocouple was a 30-gage, 2-wire, copper-constantan, glass-insulated, metal-sheathed (1/16-in. or 0.16-cm o.d.) assembly with an exposed ball junction. This thermocouple appears in figure 7 beneath the top annular window. Figure 7 also shows the vapor exit duct (supported by the annular window) and the four slip rings. Another thermocouple, which is stationary, was fabricated similar to the local fluid thermocouple; its junction was mounted just above the top slip ring to measure the exit vapor temperature. The thermocouple voltages for the circuits shown in figure 6 were read from a hand-balanced potentiometer. Other circuit details are shown in figure 6, such as the silver wire used in the local fluid thermocouple circuit between the brushes and the compensating junctions located in the vapor space near the slip rings. The assumption was made that the temperature at the slip-ring contacts, at the vapor thermocouple junction, and at the compensating junctions was the same and

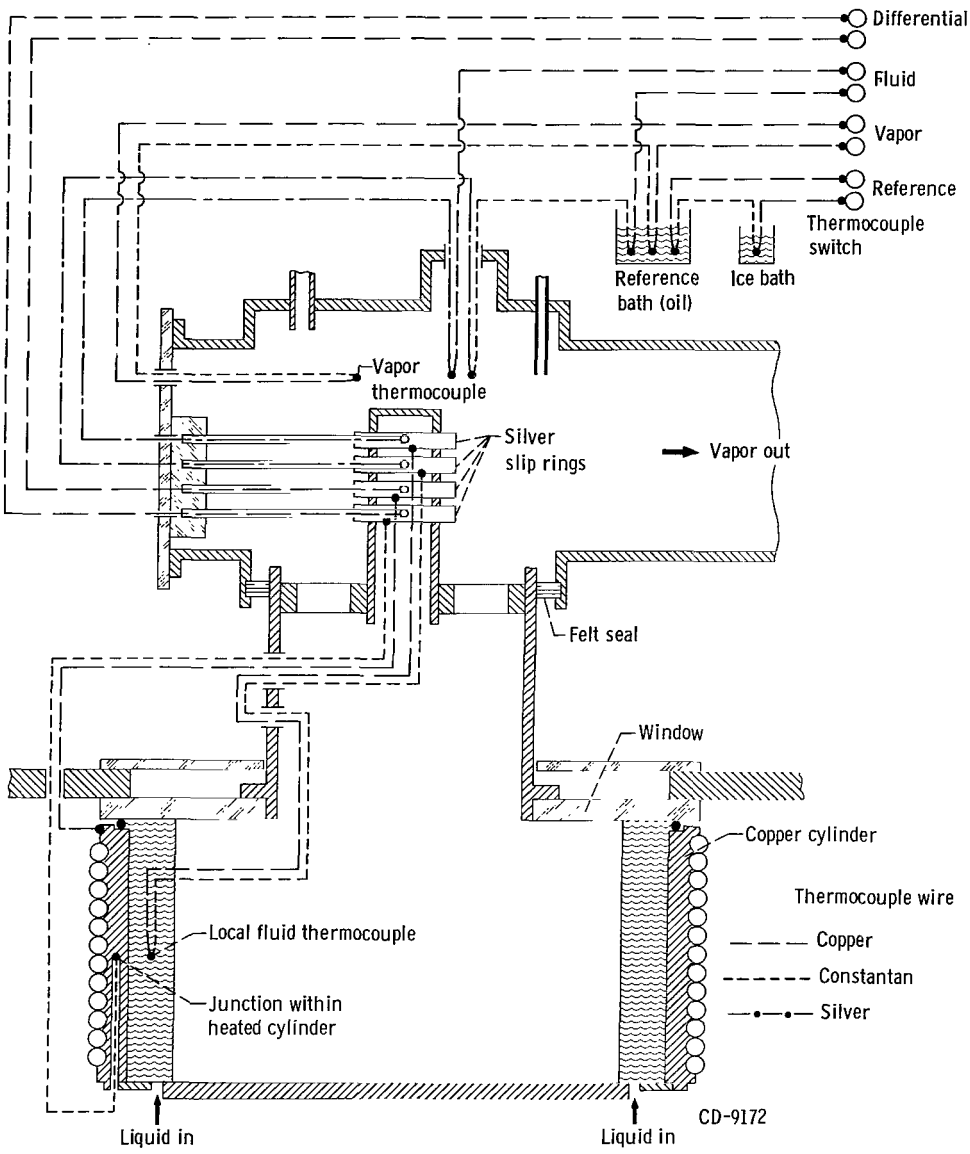

Figure 6. - Test section thermocouple circuits.

equal to the vapor saturation temperature in all the heat-transfer runs. Thus, the output of the heated-wall thermocouple circuit was a differential between the temperature at the slip-ring contacts and the soldered junction within the copper wall. The heated-wall surface temperature was obtained by calculations with known values of the copper thermal conductivity, the heat flux, and the thermocouple location.

The liquid inlet temperature was measured by a sheathed thermocouple immersed in the feed line just upstream of the rotating face seal (fig. 1). Heat flow into the boiler was measured with a wattmeter calibrated to within ±1.5 percent error.

Outlet vapor pressure was within a few inches (cm) of water of atmospheric (barometric) pressure. This small difference was measured by a ±5-inch (±12.7-cm) water

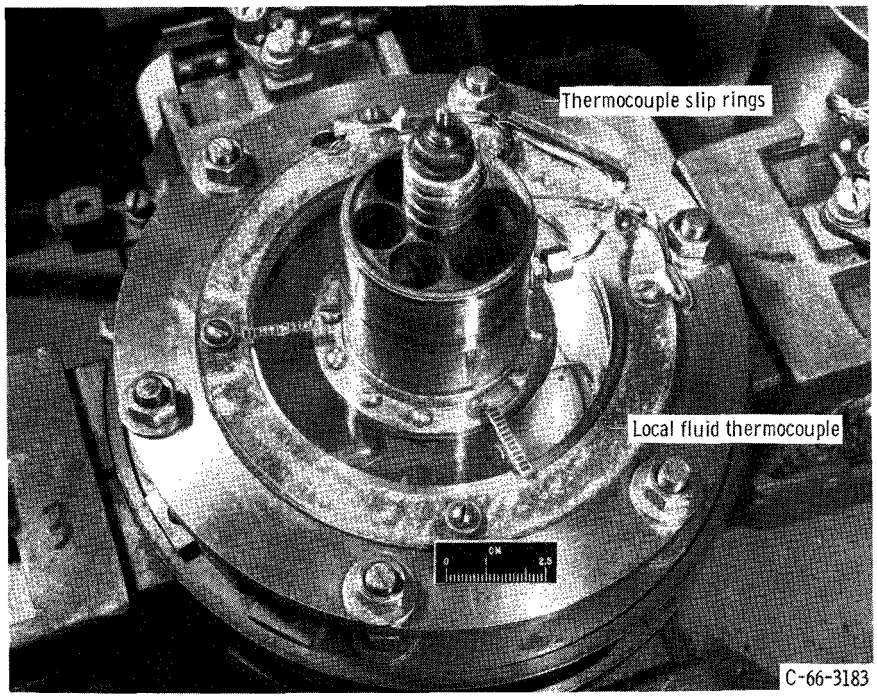

Figure 7. - Top annular window and thermocouple slip rings.

pressure gage or by a 0- to 1-inch (2.54-cm) water inclined manometer.

The boiler rotational speed was measured by a frequency counter that totaled the blips as the notched edge of the drive pulley passed by a stationary magnetic pickup. This reading was checked by an electronic strobe light used for visual observation of the boiling and for measurement of the liquid-vapor interface location. This location was determined visually to the nearest 1/16 inch (0.16 cm) with the use of scale markers attached to both the top window and to the bottom plate of the boiler.

Two types of throttling calorimeters were used. Early in the program, a small, light, NASA-built calorimeter with a 2-inch (5.1-cm) diameter and a 4-inch (10.2-cm) length was used. It contained a concentric central chamber $1\frac{3}{8}$ inches (3.5 cm) in diameter by 3 inches (7.6 cm) long with highly polished walls. The aspirated flow of vapor entered the central chamber through a 0.052-inch (0.132-cm) orifice. After the flow expanded and negotiated the baffles, it passed by temperature and pressure measurement points before exiting to a vacuum pump. The calorimeter was wrapped in glass-wool insulation and located within about 3 inches (7.6 cm) of the sampling tube entrance above the slip rings. The other calorimeter was a commercial, high-pressure type of heavy construction, approximately 6 inches (15.2 cm) in diameter by 10 inches (25.4 cm) high, with a 0.120-inch (0.305-cm) orifice and lampblack internal insulation. It was mounted about 15 inches (38 cm) from the sampling point. This calorimeter provided a check on the accuracy of the first calorimeter.

TEST PROCEDURE

Calibration

Heat loss. - To determine boiler heat losses, the inside of the boiler, including the vapor space, was packed with fiberglass insulation. The boiler was assembled exactly as for normal operation, but the water inlet valve was closed so that the boiler would be dry. The main heater was turned on, and the heat input was fixed at some low power level. The speed of the boiler was then varied at this power level. The system remained at each speed setting until thermal equilibrium was reached; the temperature of the heated-wall thermocouple was then recorded. At this equilibrium temperature, the amount of power put into the system was the same as that leaking out. It was assumed that this power was the same as the heat lost from the boiler during normal boiling operation at this same equilibrium wall temperature and speed. By repeating the procedure for different heat inputs, the heat lost was obtained as a function of rotative speed for various equilibrium wall temperatures. At 250° F (395° K) equilibrium temperature, the heat loss was never more than 120 watts. The calibrated heat loss was subtracted from the gross power input to obtain the actual heat flux through the test surface.

Thermocouples. - Considerable care was exercised in calibrating the thermocouples. The entire outside of the boiler was packed with fiberglass insulation. Saturated steam from the 5-psig (35-kN/m^2 gage) building steam line was introduced into the boiler through the feed water inlet. The steam flowed through the boiler, past the thermocouple slip-rings, and out through the condenser. The stationary thermocouple in the vapor space was accurately checked by comparing its reading with the saturation temperature calculated from the measured pressure in the vapor space.

The boiler was then rotated and the tension on the slip-ring brushes of the two rotating thermocouples was adjusted so that no frictional heating effects at the ring-brush junction could be noted on the potentiometer at speeds producing up to 200 g's. The readings of the two rotating thermocouples were then compared with that of the vapor-space thermocouple. This procedure was repeated several times, after the slip-ring assembly was dismantled and reassembled. The average deviations of the thermocouple readings from the saturated vapor temperature during the calibrations are given in the following table:

Thermocouple	Average deviation, mV
Wall	±0.009
Local fluid	±.006
Vapor	±.001

For comparison, at 220° F (378° K), a change of 0.026 millivolt corresponds to 1° F (0.556° K).

OPERATION

Just before each series of boiling runs, the test surface of the boiler was polished with 400-grit emery paper, then thoroughly cleaned with water, and wiped with a cloth saturated with a degreasing agent. Some corrosion and pitting of the tin surface occurred during operation, which made control of the surface condition very difficult. Some of this pitting is shown in figure 5.

After the boiler was cleaned and reassembled, (1) the distilled water supply tank was heated overnight to 200° F (367° K), (2) the water in the tank was boiled and vented to the atmosphere for about 15 minutes, (3) the water temperature was brought back to 200° F (367° K), (4) the tank was pressurized to about 30 psig (207 kN/m^2 gage) with nitrogen, (5) the boiler was rotated at a speed of 940 rpm (50 g's) with no heat input, and (6) the water supply valve was opened to allow water flow into the boiler. The power input to the boiler was then gradually increased until boiling commenced. The system was operated under these conditions for about 30 minutes prior to taking data.

The rotating boiler was operated quantitatively for two series of heat-transfer runs, A and B. For series A, the nominal power input was first fixed at 750 watts, and the speed of rotation was successively fixed at 515, 660, 940, 1330, and 1880 rpm (corresponding to 15, 25, 50, 100, and 200 g's at the heating surface, respectively). The power input was then increased, and the speeds were again varied in the same order. This procedure was repeated for seven power levels to 18 kilowatts. After these data runs were made, the speed of the boiler was then set to produce 25 g's, and the power input was increased in steps and then decreased.

At each value of boiler speed and power input, when thermal equilibrium was reached, the wattmeter reading was recorded and the three calibrated thermocouples were read on the potentiometer. In addition, the flow rate, liquid inlet temperature, pressure in the vapor space, calorimeter readings, and the fluid annulus thickness within the boiler were recorded.

In series B, the speed of the boiler was first set to produce 200 g's, and the power input was increased gradually in steps from 750 watts to 26 kilowatts. The speed was then set for 50 g's, and the power input was varied stepwise from 930 watts to 24 kilowatts. A similar procedure was followed for a speed of 25 g's, with the power input ranging from 930 watts to 15 kilowatts. After these data were recorded, the rotation of the boiler was stopped. With the boiler stationary, water was introduced and manually

regulated to overfill the boiler slightly while the power input was increased from 900 watts to 12 kilowatts.

High-speed motion pictures were taken during several of the test conditions for series A and B, and at other conditions, as discussed in the next section.

RESULTS AND DISCUSSION

General Performance Characteristics

Some general comments about the boiler operation are pertinent to an understanding of the data. The rotating boiler had an approximately constant volume inventory of fluid, but with a continuous through-flow, the rate of which was determined by the heating rate. At low heating rates (low flows), the boiler inventory was large relative to the inflow, and pool boiling was simulated. Because of the annular symmetry of the boiler and the several small liquid inlet holes, the boiler inventory rotated with the heated wall, in wheel flow. This condition ideally simulated pool boiling at increased gravities. At high heating rates, through-flow was larger, and at high gravities, vigorous secondary-flow cells developed in the boiling annulus as a result of convection. This subject is discussed further in the section Photographs Showing Effects of Acceleration and Heat Flux on Nucleate Boiling.

The boiler-inlet liquid temperature was also dependent on the heating rate. Because of heat losses along the feed-liquid line, the inlet liquid subcooling was considerably greater at low flow rates (low heating rates) than at high flow rates.

The liquid flow into the boiler and the vapor flow out were both steady. It was not necessary to add baffles or vanes in the boiler to correct for interface waviness or unbalance.

The rotative centrifugal accelerations, expressed herein as gravities, are those acting normal to the heated cylindrical wall; the earth gravity vector is neglected. At accelerations below about 25 g's, the parabolic shape of the liquid-vapor interface became observable. Above 25 g's, the interface in the boiler was essentially a cylindrical, vertical surface concentric with the heated surface. Therefore, above 25 g's, the boiler should be insensitive to its orientation to earth gravity.

Below about 14 g's, a constant fluid thickness could not be maintained during the boiling process, and data were not obtained. Part of this trouble was caused by corrosion which permitted liquid to leak into the hollow float; this leakage was discovered later and corrected. At all accelerations above 14 g's and at all flow rates, the float valve worked well.

In general, comments pertaining to the boiling action and the two-phase flow mecha-

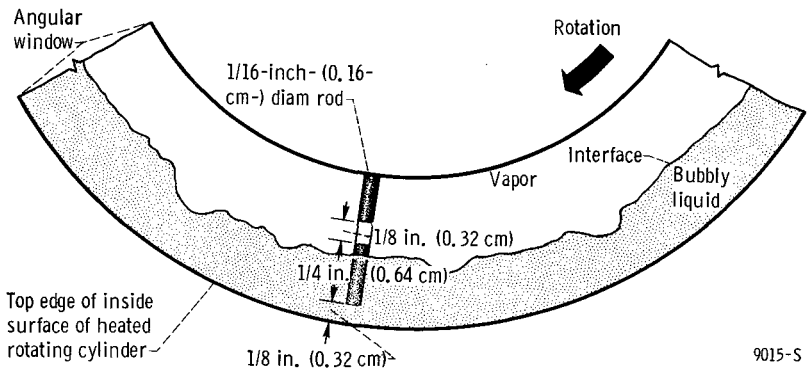

Figure 8. - Sketch showing typical view through top annular window.

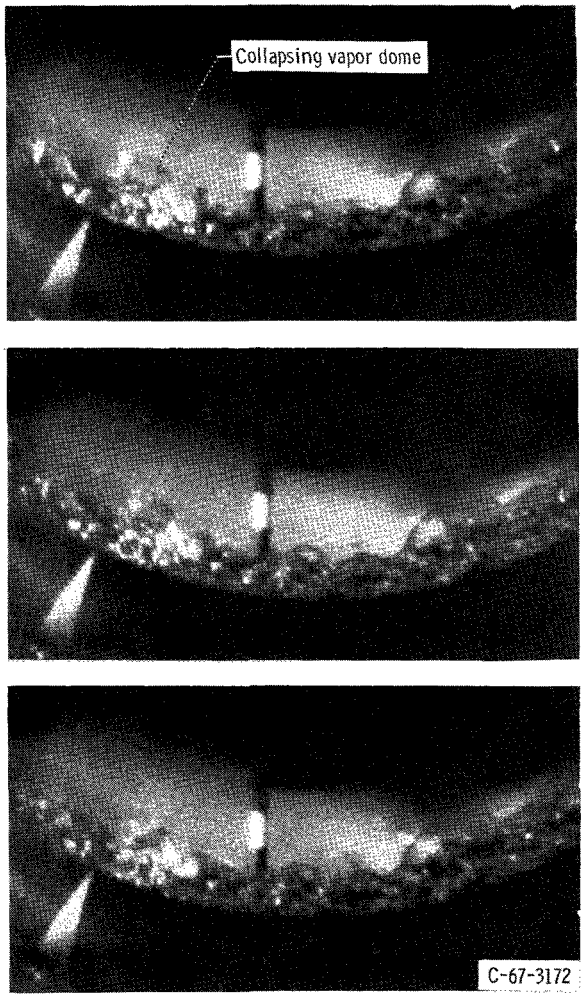

Figure 9. - Sequence of three consecutive frames from high-speed motion picture showing boiling and collapse of vapor dome at 25 g's and heat flux of 88 000 Btu per hour per square foot (0.28 MW/m^2).

nisms are based on careful study of the high-speed motion pictures, most of which were taken in color to provide good contrast and definition to the bubbles, interface, and droplets in the vapor space. The principal features to be seen in a typical frame from a high-speed motion picture taken through the top annular window are shown in figure 8. The outer circular arc is the edge (end view) of the heated cylinder. The thin annulus of boiling fluid lies against this heated surface. Vapor bubbles form at the heated wall and move radially inward to break at the interface. The 1/16-inch- (0.16-cm-) diameter rod shown in most of the subsequent photographs turns with the boiler. For visualization and scale purposes, this rod is painted dark red with a white central band 1/8 inch (0.32 cm) long. The rod is oriented horizontally 1/4 inch (0.64 cm) below the top window and is alined almost in a radial direction.

The boiling annulus for a typical condition at 25 g's is shown in figure 9 by three consecutive frames from a 16-millimeter motion picture taken at about 8000 frames per second. The heat flux was 88 000 Btu per hour per square foot (0.28 MW/m^2). The interface is very irregular and turbulent at this gravity level. Many times, several vapor bubbles or clusters are pumped into a certain region, and upon reaching the interface, balloon into large vapor "domes" before breaking. The dome to the left of the rod in figure 9 (top) is breaking open (from the left) to let out the vapor. The liquid that forms the roof of the dome can be seen (center and bottom) pulling together into a ring of droplets that fall back into the interface. Occasionally, a drop or stream of liquid is propelled far into the vapor region beyond the interface. This liquid generally returns to the interface after completing an arcing trajectory. This interface activity is clearly shown in the film supplement described at the back of this report and available on loan.

Boiling Heat Transfer

The experimental boiling heat-transfer data are presented in chronological order in table I. Symbols are defined in the appendix.

Heat-flow balance. - A check on the boiler overall heat-transfer and flow instrumentation is given in figure 10. Here, the measured gross electrical power into the boiler is compared with the thermal power calculated as follows:

$$\text{Thermal power} = K_1 W_\ell \left[L + (T_{sat,\,v} - T_{\ell,\,in}) C_p \right] \qquad \text{Btu/hr; kW}$$

where K_1 is 1; 0.293×10^{-3}. This expression accounts for the sensible heat required to overcome inlet liquid subcooling and the heat required to evaporate all the inlet liquid flow (as determined by the flowmeter). The agreement shown in figure 10 between the calculated and measured power is always within 10 percent error, except at the lowest

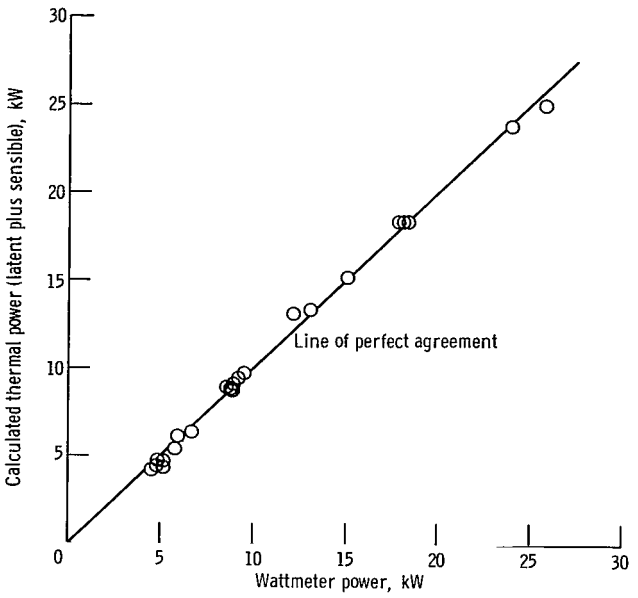

Figure 10. - Heat and flow balance for rotating boiler.

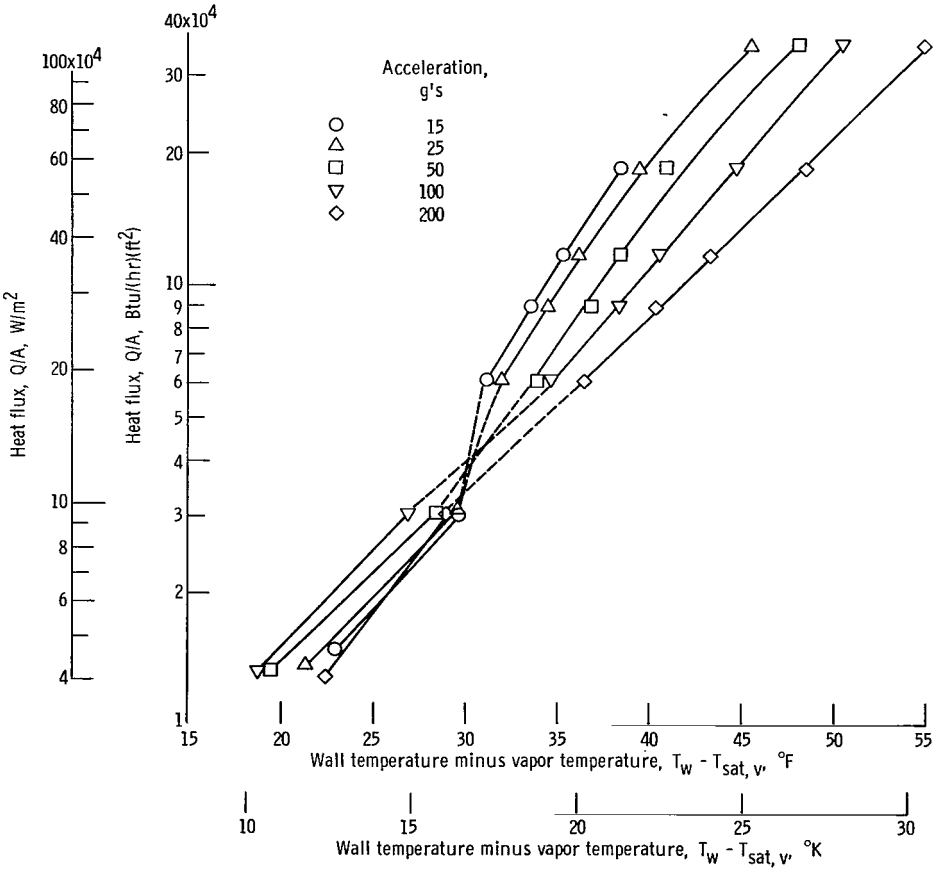

Figure 11. - Boiling heat-transfer data for series A runs.

flows. At flows below about 14 pounds per hour (6.4 kg/hr), the flowmeter was erratic and data were not recorded. Most of the data are within ±3 percent error.

Effect of acceleration on boiling. - The effect of rotational acceleration on boiling heat transfer is shown in figure 11. Heat flux is plotted against the differential between wall temperature and the saturation temperature measured in the vapor space $T_{sat, v}$. Data from series A runs are shown for five levels of acceleration. Note that the acceleration effects are reversed at a heat flux of about 45 000 Btu per hour per square foot (0.14 MW/m^2). This result agrees with the data of Merte and Clark (ref. 2). At heat fluxes greater than 60 000 Btu per hour per square foot (0.19 MW/m^2), an increase in

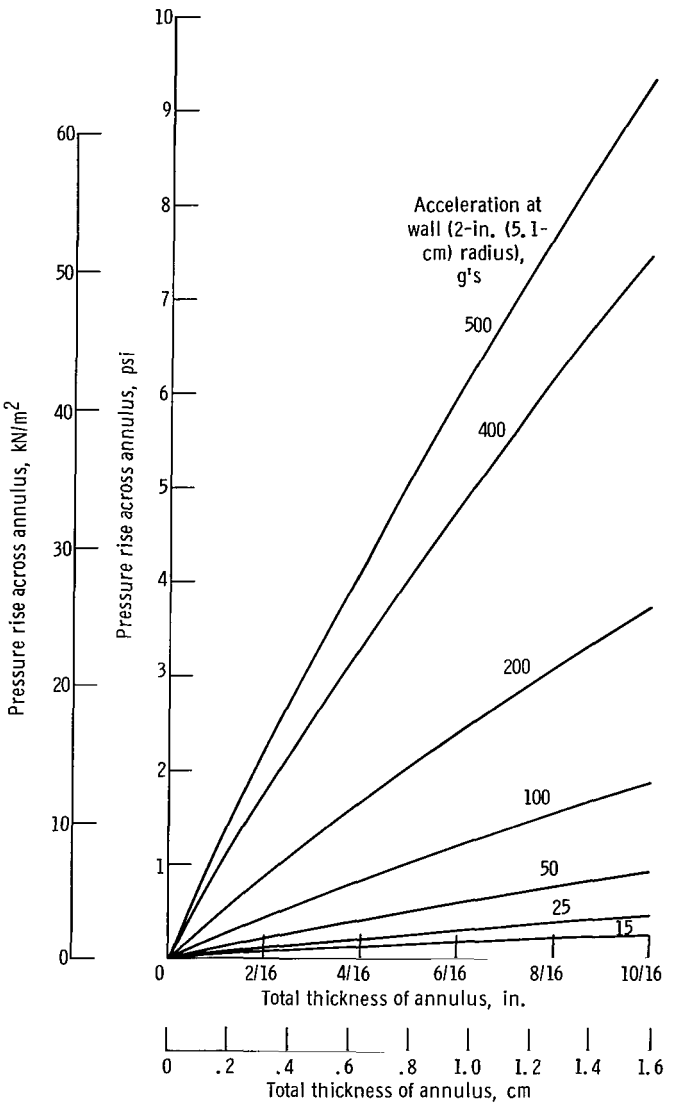

Figure 12. - Pressure rise across liquid annuli of various thicknesses within 4-inch- (10.2-cm-) diameter rotating cylinder. Saturated water at 1 atmosphere (0.101 MN/m^2).

acceleration increases the temperature differential $T_w - T_{sat, v}$. Thus, at any given wall superheat above vapor temperature, an increase in acceleration decreases the rate of heat transfer. The trend in the low heat-flux region (where natural convection is important) is generally opposite to that just described. As the acceleration is increased, the rate of transfer improves (data at 200 g's are an exception).

The data shown in figure 11 do not account for the pressure rise across the thickness of the boiling annulus from the vapor space to the boiler wall. This pressure rise is shown in figure 12 for various thicknesses of liquid annuli and for various accelerations. The pressure rises of figure 12 were used to calculate the saturation temperature at the boiler wall $T_{sat, w}$. The data of figure 11 are replotted in figure 13 against the temperature differential $T_w - T_{sat, w}$. In addition, the average amount of subcooling for each acceleration is given. All the data have now been shifted to lower wall superheats than those of figure 11 because $T_{sat, w}$ is higher than $T_{sat, v}$. The boiling fluid annulus was assumed to be liquid in these calculations because the true fluid densities (or void frac-

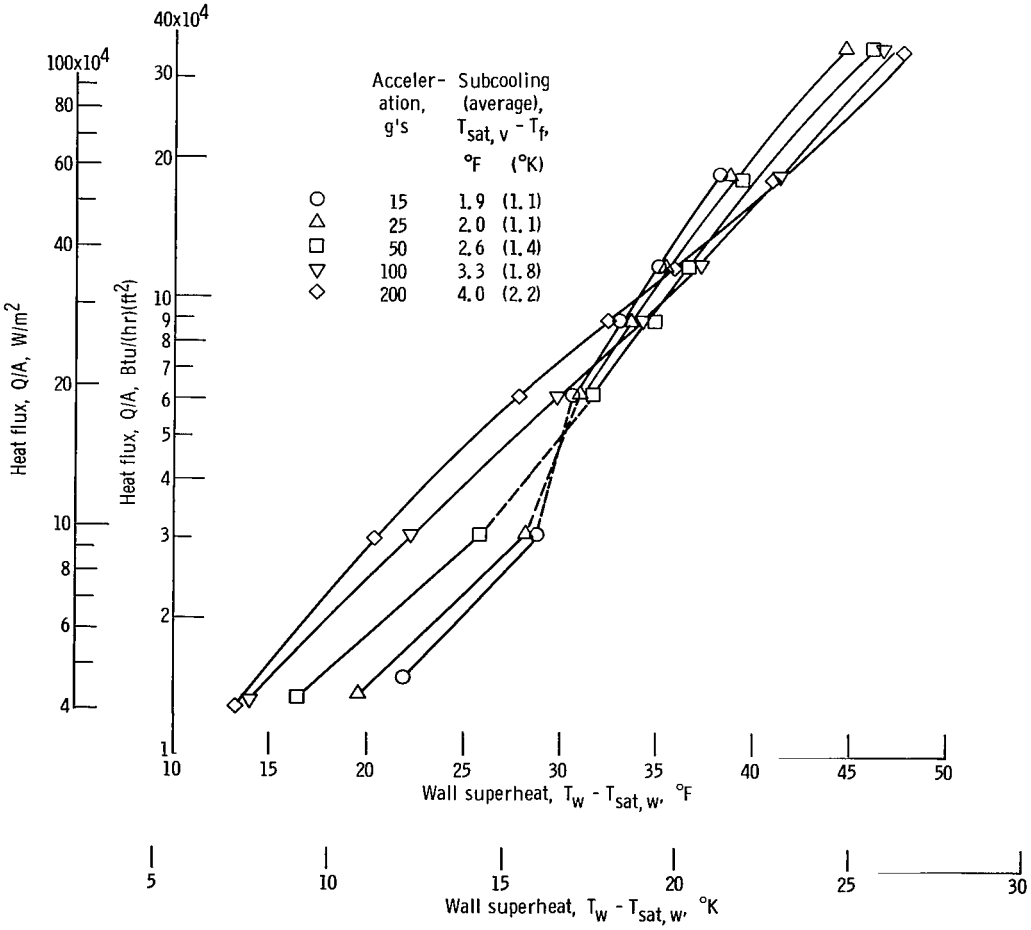

Figure 13. - Effect of gravity on heat flux as function of wall superheat for series A data.

tions) were not known. The assumption of all-liquid in the annulus resulted in some overcorrection of the data; this error is worse at the high heat fluxes and at the low gravities (greatest voids). However, at the low gravities the pressure rise in the fluid is small, so that this error due to density is minor. The results shown in figure 13 give a better indication of the acceleration trends and agree with those of Merte and Clark (ref. 2).

In the low heat-flux region, natural convection is important and gravity increases the heat transfer. In the high heat-flux region, the gravity trend is reversed, although small in magnitude. An increase in acceleration decreases the heat flux. Both Merte and Clark (ref. 2) and Costello and Tuthill (ref. 3) discuss this phenomenon. They postulate that, since an increase in acceleration reduces bubble size and since the bubbles are responsible for transferring the heat (whether by agitation or latent transport), then as the acceleration is increased, the heat flux will decrease.

The crossover point of 45 000 Btu per hour per square foot (0.14 MW/m^2) is no longer meaningful as it was in figure 11. In fact, the 200-g line does not complete its crossover until above 175 000 Btu per hour per square foot (0.55 MW/m^2).

Graham and Hendricks (ref. 4) have shown that, as the acceleration increases, the threshold temperature and heat flux for nucleation (the incipient point) also increases. With these points in mind, the reversal trend in the data may be schematically postulated, as shown in the following sketch.

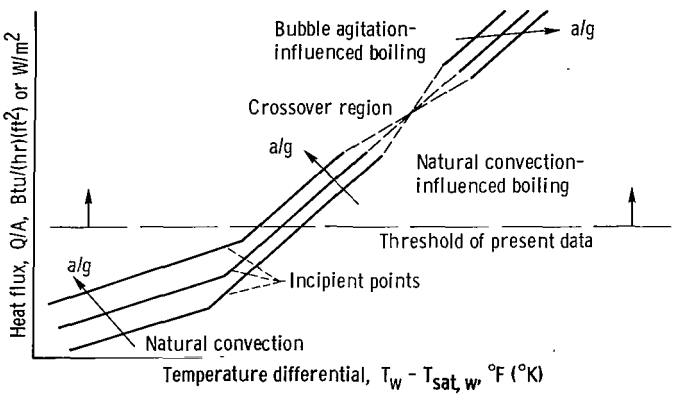

Adelberg (ref. 8), Keshock and Siegel (ref. 9), and Graham and Hendricks (ref. 4) consider the various forces (inertia, buoyancy, and surface tension) that act on the bubbles during the nucleation process. Adelberg postulates that, for various fluids at different gravity levels and superheats, some of these forces may be more dominant than others. If the buoyancy forces are large compared with the other forces, gravity effects will be measurable. On the other hand, if buoyancy forces are small, the gravity effects may be negligible. A consideration of these forces may be necessary to determine when the adverse gravity effect on boiling will begin to cancel the positive gravity effect on natural convection. In other words, the crossover points in the data may vary with

the fluid, gravity level, and wall superheat.

Reproducibility of data. - Figure 14 compares the data of figure 13 taken at an acceleration of 25 g's with that of run 8, series A, also taken at 25 g's. The open symbols were taken at a constant heat flux Q/A and variable accelerations. The solid symbols were taken at a constant acceleration and variable Q/A (first increasing, then decreasing). The latter data were taken after the boiler had operated for 7 hours.

In addition to normal data scatter and any aging effects of the boiler surface, the comparison shown in figure 14 includes two other effects. First, the two curves represent different procedures for obtaining data, which resulted in different values of inlet liquid subcooling for comparable data points (see table I), even though the average of the local fluid subcoolings was nearly the same in the two cases (2.0° F or 1.1° K and 1.8° F or 1° K). Also, the data taken at a constant g (solid symbols) were subject to variations from the oft observed boiling hysteresis effect (e.g., see fig. 9 of ref. 10).

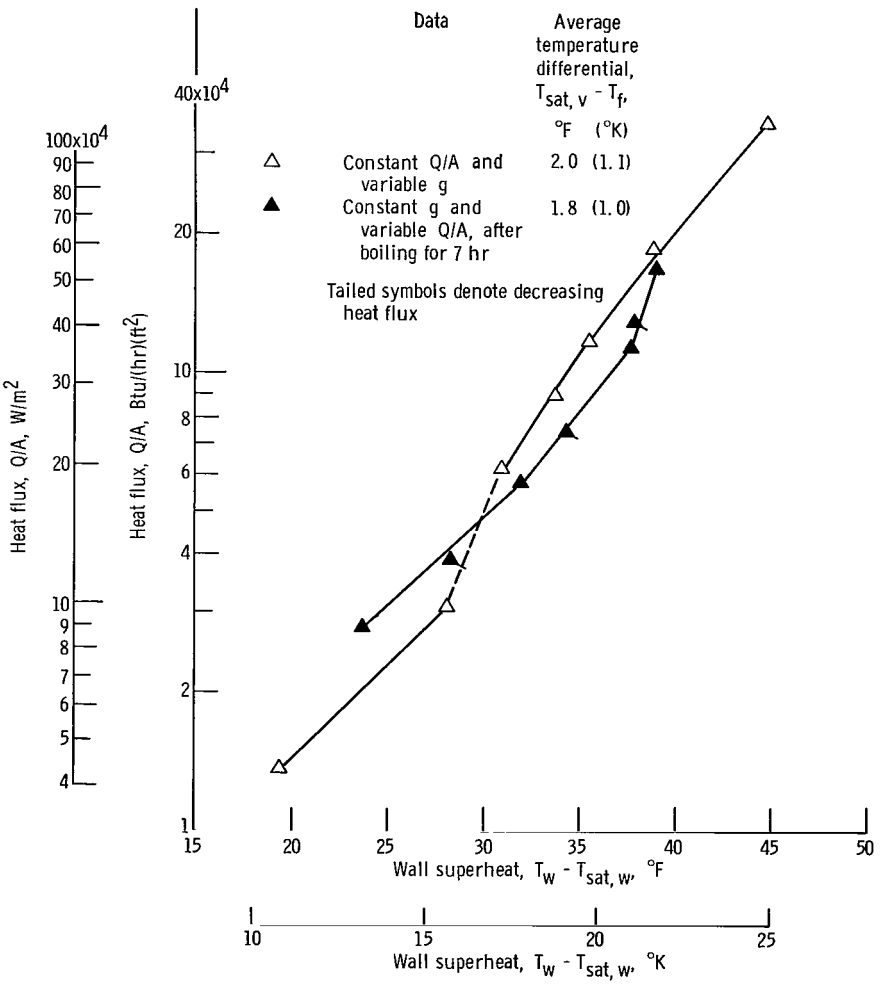

Figure 14. - Repeatibility of heat-transfer data for series A at 25 gravities.

With these effects considered, the repeatability shown in figure 14 is fairly good.

The data of series B runs repeat many of the test conditions of series A, except that series B was run in the mode of constant acceleration and increasing heat flux between successive data points. Prior to series B runs, the boiler was dismantled, and the test surface was repolished and cleaned. Series B data are shown in figure 15. Data are also shown for the boiler not rotating.

The trends in figure 15 are similar to those of the series A data (fig. 13), but more wall superheat is now required in the high heat-flux region. This result is believed due to the pitting and possible corrosion of the boiler test surface that occurred after the runs of series A. The effects of surface conditions, such as pits and crevices, on wall superheat during boiling is well known (ref. 11). The increased data scatter in figure 15 compared with that of figure 13 is partly attributable to the more variable inlet liquid temperature (caused by thermal losses and lag in the feed line coupled with the series B mode of increasing heat flux). The effects of acceleration on heat transfer are judged to be more accurately and clearly shown by the series A data than by those of series B. It is noteworthy that wall superheat variations at high heat fluxes are as large because of unresolved effects, such as surface conditioning and aging, as they are because of grav-

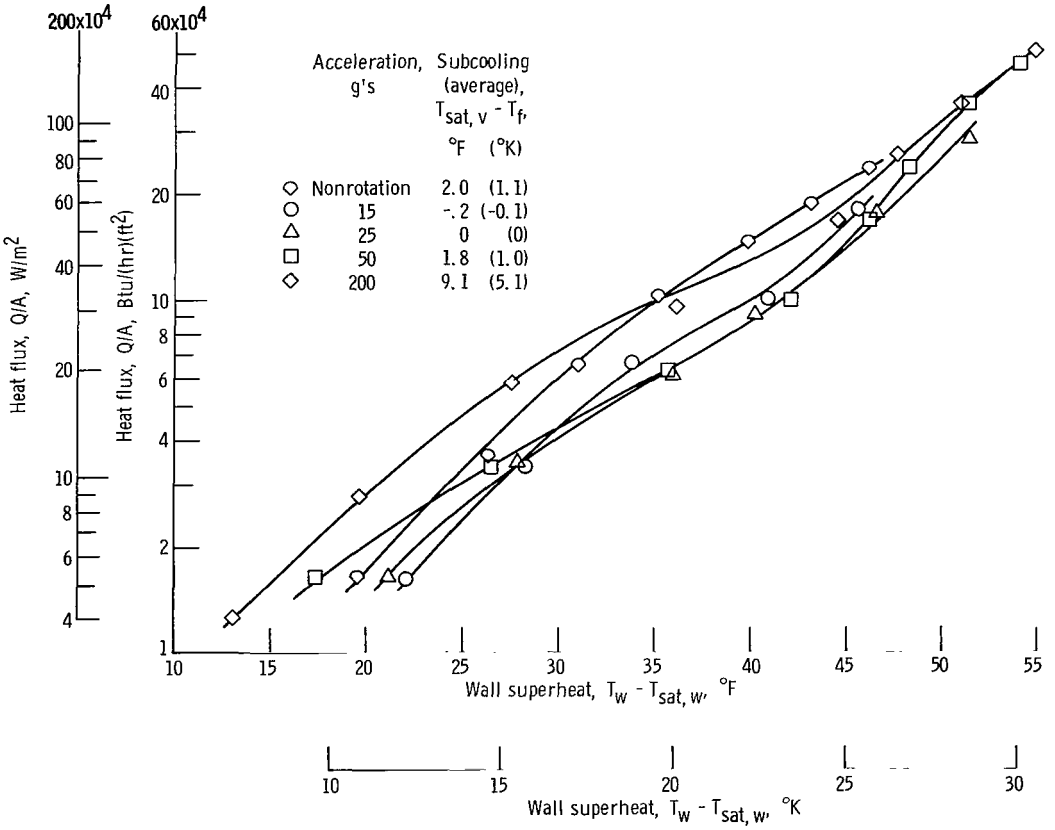

Figure 15. - Heat flux as function of wall superheat for series B runs, including nonrotation.

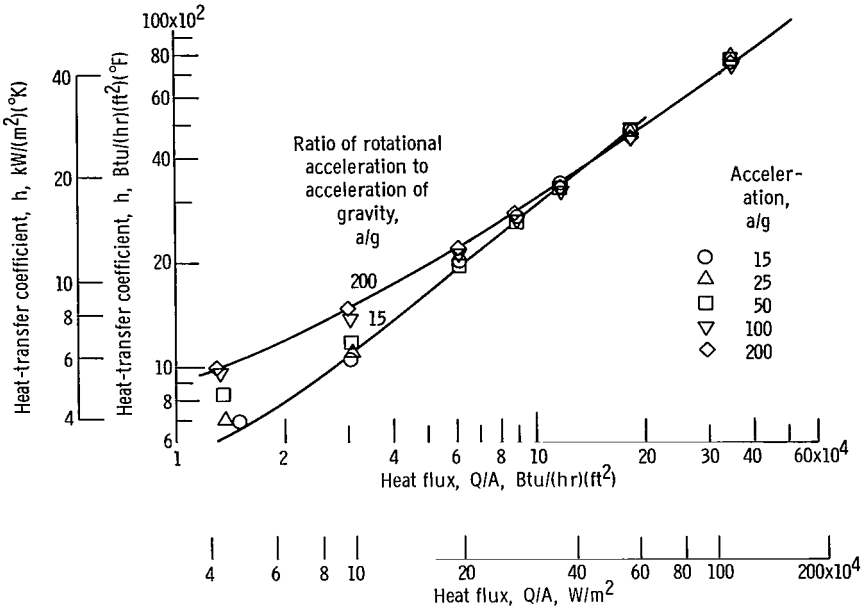

Figure 16. - Boiling heat-transfer coefficients for series A data.

ity changes from 1 to 200.

Heat-transfer coefficients. - The boiling heat-transfer coefficients h for the series A data are shown in figure 16. These coefficients are defined as $Q/[A(T_w - T_{sat,w})]$. At high heat-flux levels, the coefficients for all gravities fall into a narrow band that increases with heat flux at about the 0.8 power. At low heat fluxes, where boiling is convection dominated, increasing acceleration substantially increases the coefficients.

Local fluid temperature. - Because of the heat losses along the supply line, the inlet liquid temperature increased as the flow rate increased. The data in table I show that the measured local fluid temperature in the boiler responded to the inlet liquid temperature; high values of the inlet liquid temperature produced high values of the measured local fluid temperature for comparable conditions. However, the local fluid temperature can also be seen to vary as a result of acceleration, as shown in figure 17. A high and low gravity case are compared at both a low and a high heat-flux condition. The cases shown have nearly identical inlet liquid temperatures for the two g levels. (The variations in interface locations depended on the float valve operation and are not deemed significant.) Figure 17 shows what information is known along a radius line normal to the heated wall at the boiler midpoint; namely, wall temperature, fluid temperature 1/8 inch (0.32 cm) inward from the wall, interface location, vapor saturation temperature, and calculated liquid saturation temperature. Connecting the known temperatures with a probable curve reveals an interesting situation: a temperature "inversion" exists above the heated thermal layer and becomes more pronounced at higher g's. Logically,

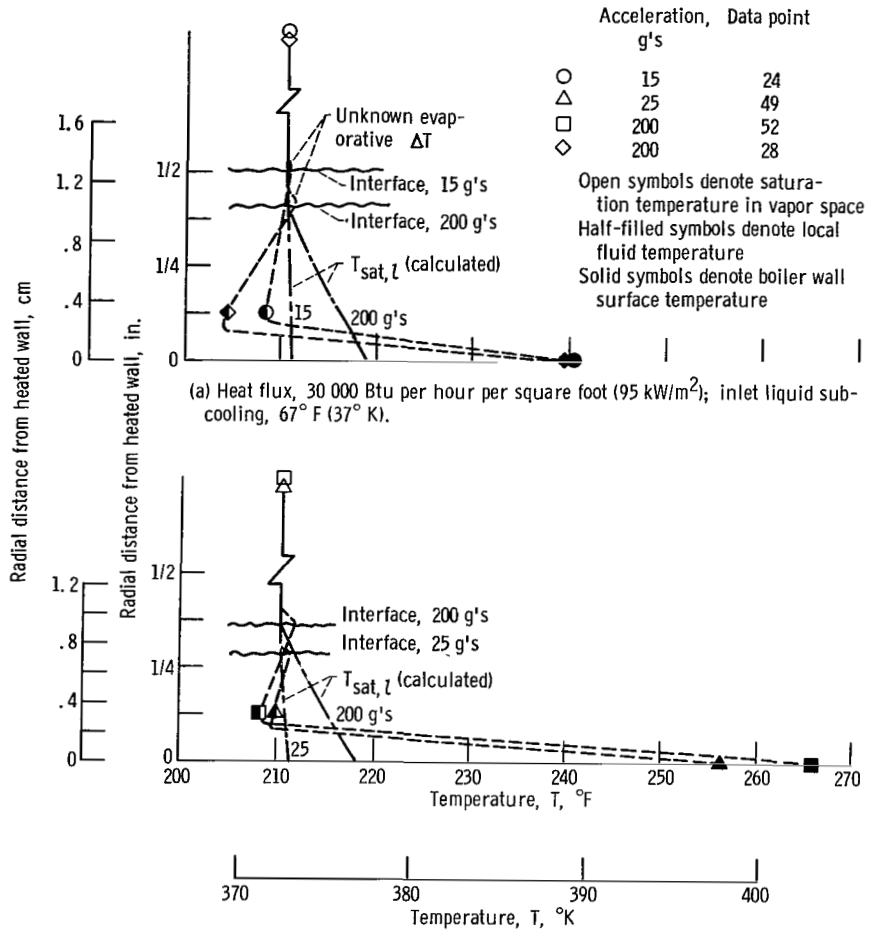

(a) Heat flux, 30 000 Btu per hour per square foot (95 kW/m^2); inlet liquid subcooling, 67° F (37° K).

(b) Heat flux, 350 000 Btu per hour per square foot (1.1 MW/m^2); inlet liquid subcooling, 20° to 22° F (11° to 12° K).

Figure 17. - Postulated radial temperature distributions in rotating boiler.

the colder, denser elements of fluid will be centrifuged to the outer radii. But the heat transport has to act against this effect. Two mechanisms that might accomplish this are (1) heat transport by discrete vapor bubbles distributed rather uniformly through the fluid and buoyed up rapidly to the interface and (2) heat transport by warm liquid in convective secondary-flow cells (with updrafts and downdrafts) and direct evaporation from the hotter liquid at the free interface. The action observed in this study indicates that both mechanisms are operating, with low gravity conditions approaching case (1) and high gravity approaching case (2). Since most of the local fluid temperature readings are lower than the vapor temperature, it could be concluded that the fluid temperature probe was located in a convective downdraft, or perhaps in a current from a liquid-feed hole. However, the fluid temperature is not always colder than the vapor. At low g's and high heating rates, the local fluid temperature exceeded the vapor temperature frequently, and in six cases, the fluid temperature was slightly higher than the saturated

liquid temperature at the wall. Photographs of the boiling annulus presented in the next section yield additional information on this subject.

Photographs Showing Effects of Acceleration and Heat Flux on Nucleate Boiling

The effect of acceleration on nucleate boiling can be seen by comparing figure 9 with the sequence shown in figure 18. The photographs were all taken at the same heating rate of 88 000 Btu per hour per square foot (0.28 MW/m^2), but at steadily increasing g's up to 400 (fig. 18(d)). The bubble size and number markedly decrease, and the interface becomes more continuous and smooth at higher g's. At 400 g's, the fluid in the annulus is mostly clear liquid with only an occasional cluster of bubbles. The rod can be seen

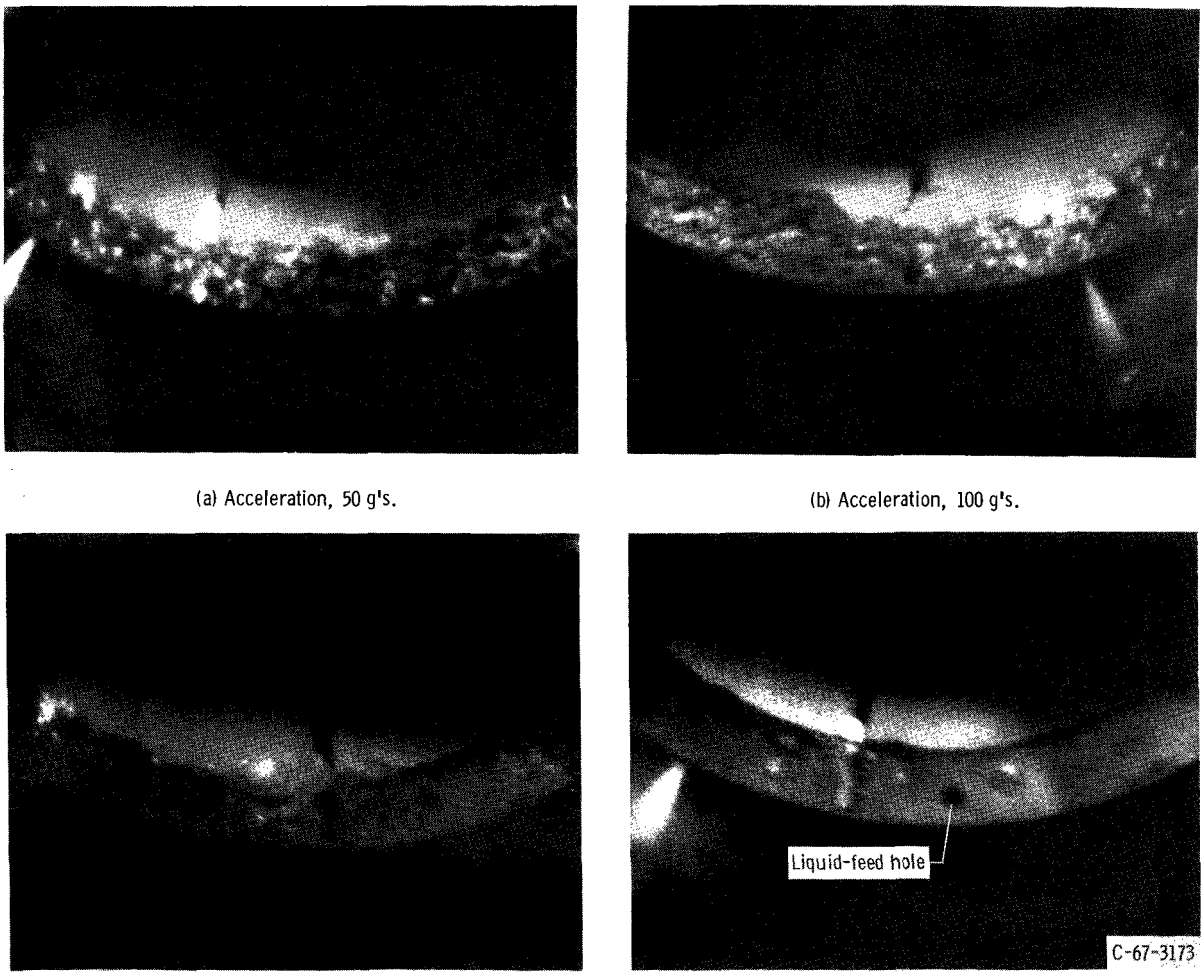

(a) Acceleration, 50 g's.

(b) Acceleration, 100 g's.

(c) Acceleration, 200 g's.

(d) Acceleration, 400 g's.

Figure 18. - Effect of increasing gravity on boiling at constant heat flux of 88 000 Btu per hour per square foot (278 KW/m^2).

easily as can the liquid-feed holes (dark spots) in the bottom plate of the boiler. Figures 18(c) and (d) show the typical bubble patterns at high g's - clusters of bubbles separated by relatively clear liquid. This pattern strongly suggests that secondary-flow convective cells exist, with the bubbles appearing in the warmer updrafts. So few bubbles exist at the highest g's, however, that transport of all the heat by vapor bubbles alone appears very doubtful. Direct evaporation at the interface must also occur. This secondary flow and evaporation process is illustrated and discussed in the motion picture supplement to this report.

Boiling at a low heat flux (17 400 Btu/(hr)(ft^2) or 55 kW/m^2) is illustrated in figures 19(a) and (b) at 25 and 100 g's, respectively. Figure 19(a) shows two consecutive frames. At 100 g's (fig. 19(b)), individual bubbles and chains of bubbles can be seen easily. It appears that the bubbles, on nearing the interface, grow larger, agglomerate, and spread out laterally along the interface as they break.

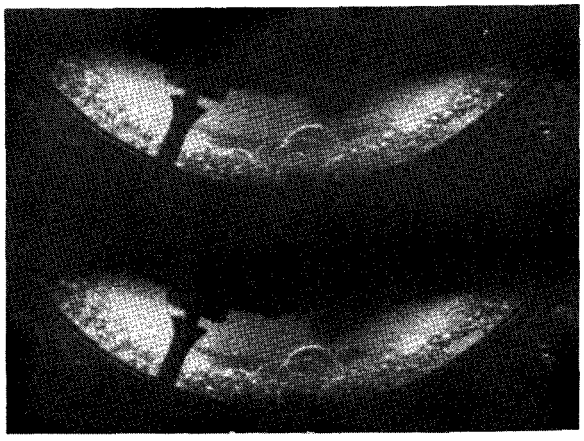

(a) Acceleration, 25 g's.

(b) Acceleration, 100 g's.

Figure 19. - Boiling at low heat flux of 17 400 Btu per hour per square foot (55KW/m^2).

(a) Acceleration, 100 g's.

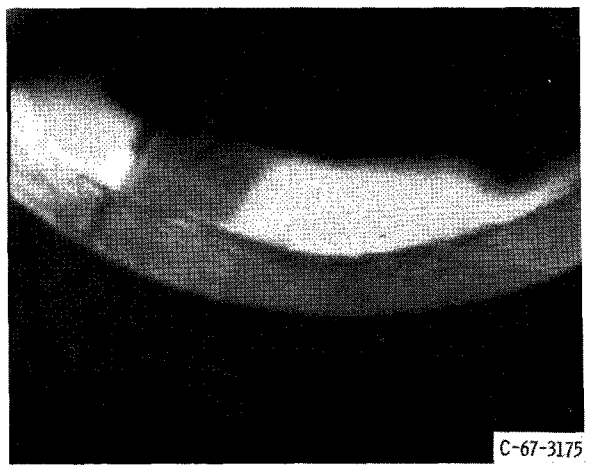

(b) Acceleration, 400 g's.

Figure 20. - Boiling at high heat flux of 468 000 Btu per hour per square foot (1.5 MW/m^2).

A high-heat-flux case (468 000 $Btu/(hr)(ft^2)$ or 1.48 MW/m^2) is shown in figure 20. At 100 g's, the fluid in the boiling annulus appears almost foamy (fig. 20(a)). The rod cannot be seen through 1/4 inch (0.64 cm) of boiling fluid. At 400 g's (fig. 20(b)), the rod can be seen, as well as many areas of clear liquid. This heat flux is comparable to or above a normal burnout condition for pool boiling at 1 g (ref. 12). Previous experimenters (refs. 6 and 7) have established that the burnout heat flux increases with gravity approximately to the one-fourth power. No burnout conditions were attempted in this investigation.

The effect of heat flux on boiling at 100 g's can be seen by comparing figure 20(a) at 468 000 Btu per hour per square foot (1.48 MW/m^2), figure 18(b) at 88 000 Btu per hour per square foot (0.28 MW/m^2), and figure 19(b) at 17 400 Btu per hour per square foot (55 kW/m^2).

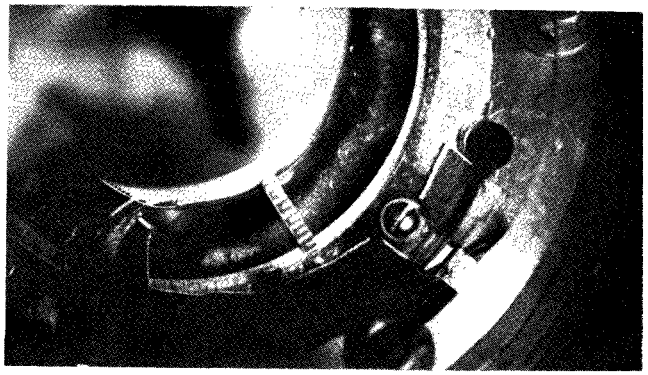

(a) Acceleration, 73 g's.

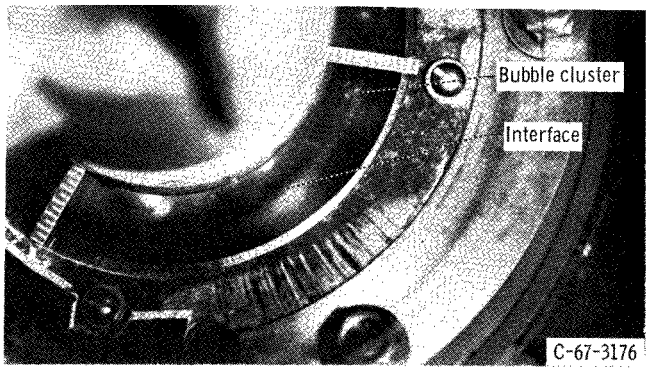

(b) Acceleration, 475 g's.

Figure 21. - Short-duration flash photographs of boiler in operation at heat flux of 117 000 Btu per hour per square foot (0.37 M W/m^2).

Flash pictures of the boiler with a 1-microsecond duration are shown in figure 21 for a heat flux of 117 000 Btu per hour per square foot (0.37 MW/m^2). At 73 g's, a continuous cloud of bubbles is apparent along the interface (fig. 21(a)), whereas at 475 g's (fig. 21(b)), one isolated cluster of bubbles appears (at 3 o'clock). Elsewhere, the interface is a thin gray line.

Unquestionably, interface disturbances were reduced and smoothed out by high accelerations. The bubbles and voids were much less numerous and appeared smaller at higher g's. Apparently, acceleration can be increased to overcome and suppress boiling at any conventional boiling heat flux level.

Exit Vapor Quality

Table I gives readings of outlet vapor quality as determined by two calorimeters. The qualities are slightly conservative because of heat losses from the calorimeters. A quality reading of 99.8 percent was obtained (data points 8 and 9) at a time when the outlet vapor temperature was 5° to 8° F (3° to 4.5° K) above the vapor saturation tempera-

ture. (Except for five marked cases of exit vapor superheat, the measured outlet vapor temperatures agreed with the saturated vapor temperatures calculated from measured outlet vapor pressures within $\pm 0.1^{\circ}$ F ($\pm 0.06^{\circ}$ K).) The commercial calorimeter was slightly more conservative in this installation than the smaller NASA Lewis calorimeter and had a greater thermal lag, which made it less sensitive to changes in test conditions.

The exit vapor quality was always above 99 percent. The quality apparently increased with gravity and liquid inlet temperature, and it decreased with heating rate.

Evidence of vapor superheat is remarkable. The vapor outflow could not come in contact with the heated surface, as it may do in conventional boiler tubes near the exit where the liquid film does not completely cover the tube wall. At high accelerations, vapor apparently could leave the interface at temperatures several degrees above the vapor saturation temperature, probably as a result of the pressure rise within the boiling annulus. For example, at 400 g's, the liquid saturation temperature at the boiler wall was 10.4° F (5.8° K) hotter, for a 1/4-inch- (0.64-cm-) thick annulus of water, than at the interface (corresponding to a pressure rise of 3.3 psi or 22.8 kN/m^2, fig. 12). The hotter liquid and vapor created near the heated wall was probably centrifuged quickly to the interface, and evaporation occurred directly across the sharp interface discontinuity. Ultimately, as gravity increases and the heating rate is held constant, all the vapor is generated by evaporation at the interface, and boiling is suppressed.

SUMMARY OF RESULTS

Over the range of variables covered in this investigation of acceleration effects in a cylindrical rotating boiler with continuous through-flow of fluid, the following principal results were obtained:

1. Stable boiling of water with outlet vapor qualities always above 99 percent was achieved at accelerations to 475 g's and heat fluxes up to 505 000 Btu per hour per square foot (1.59 MW/m^2).

2. Boiling heat-transfer coefficients up to 9000 Btu per hour per square foot per $^{\circ}$F (51 $kW/(m^2)(^{\circ}K)$) were obtained. Increased acceleration increased the heat-transfer coefficients at low heat fluxes and decreased them slightly at high heat fluxes, in agreement with previous experimenters. However, the "crossover" region occurred at progressively higher flux levels for higher accelerations. Unresolved effects, such as surface conditioning and aging, affected the coefficients at high heat fluxes as much as did gravity variations from 1 to 200.

3. Temperature and high-speed photographic data point strongly toward a well-developed secondary-flow convection cell pattern in the boiler at high g's. The few bub-

bles present at high gravity levels were small and clustered, with relatively clear liquid between the clusters. The interface became continuous, smooth, and stable and was postulated to transfer much of the total heat flux by direct evaporation into the vapor space.

4. The vertical axis of rotation of the boiler produced a paraboloidal liquid-vapor interface that appeared cylindrical at accelerations of 25 g's and above; consequently, above 25 g's, the boiler should be insensitive to its orientation to earth gravity.

5. The good performance of the rotating boiler warrants its consideration in a variety of Rankine cycle systems for power generation.

Lewis Research Center,
National Aeronautics and Space Administration,
Cleveland, Ohio, August 23, 1967,
120-27-02-03-22.

APPENDIX - SYMBOLS

A	area, ft^2; m^2
a/g	ratio of rotational acceleration to acceleration of gravity
C_p	specific heat, Btu/(lb)(^oF); J/(kg)(^oK)
g	acceleration due to gravity, 32.2 ft/sec^2; 9.8 m/sec^2
h	boiling heat-transfer coefficient $Q/[A(T_w - T_{sat,w})]$, Btu/(hr)(ft^2)(^oF); W/(m^2)(^oK)
L	latent heat of vaporization, Btu/lb; J/kg
P	pressure, in. of mercury absolute; N/m^2
$P_{v,e}$	exit vapor pressure, in. of mercury absolute; N/m^2
Q/A	heat flux, Btu/(hr)(ft^2); W/m^2
T	temperature, ^oF; ^oK
T_f	local fluid temperature, ^oF; ^oK
$T_{l,in}$	inlet liquid temperature, ^oF; ^oK
$T_{sat,v}$	saturation temperature in vapor space, ^oF; ^oK
$T_{sat,w}$	saturation temperature at boiler wall, ^oF; ^oK
$T_{v,e}$	measured exit vapor temperature, ^oF; ^oK
T_w	boiler wall surface temperature, ^oF; ^oK
W_l	liquid flow rate, lb/hr; kg/hr

REFERENCES

1. Gray, Vernon H.: Feasibility Study of a Rotating Boiler for High-Performance Rankine Cycle Power Generation Systems. Paper presented at the Intersociety Energy Conversion Conference, Miami Beach, Aug. 13-17, 1967.

2. Merte, Herman, Jr.; and Clark, J. A.: Pool Boiling in an Accelerating System. J. Heat Transfer, vol. 83, no. 3, Aug. 1961, pp. 233-242.

3. Costello, C. P.; and Tuthill, W. E.: Effects of Acceleration on Nucleate Pool Boiling. Chem. Eng. Progr. Symp. Ser., vol. 57, no. 32, 1961, pp. 189-196.

4. Graham, Robert W.; and Hendricks, Robert C.: A Study of the Effect of Multi-G Accelerations on Nucleate-Boiling Ebullition. NASA TN D-1196, 1963.

5. Beckman, W. A.; and Merte, H., Jr.: A Photographic Study of Boiling in an Accelerating System. Paper No. 64-WA/HT-29, ASME, 1964.

6. Costello, C. P.; and Adams, J. M.: Burnout Heat Fluxes in Pool Boiling at High Accelerations. Mech. Eng. Dept., Univ. Wash., 1960.

7. Ivey, H. J.: Preliminary Results on the Effect of Acceleration on Critical Heat Flux in Pool Boiling. Rep. No. AEEW-R-99, United Kingdom Atomic Energy Authority, 1961.

8. Adelberg, M.: Effect of Gravity Upon Nucleate Boiling. Physical and Biological Phenomena in a Weightless State. Vol. 14 of Advances in the Astronautical Sciences. Elliott T. Benedikt and Robert W. Halliburton, eds., Western Periodicals Co., 1963, pp. 196-222.

9. Keshock, Edward G.; and Siegel, Robert: Forces Acting on Bubbles in Nucleate Boiling Under Normal and Reduced Gravity Conditions. NASA TN D-2299, 1964.

10. Jeglic, Frank A.; Stone, James R.; and Gray, Vernon H.: Experimental Study of Subcooled Nucleate Boiling of Water Flowing in 1/4-inch-Diameter Tubes at Low Pressures. NASA TN D-2626, 1965.

11. Marto, P. J.; and Rohsenow, W. M.: Effects of Surface Conditions on Nucleate Pool Boiling of Sodium. J. Heat Transfer, vol. 88, no. 2, May 1966, pp. 196-204.

12. Tong, L. S.: Boiling Heat Transfer and Two-Phase Flow. John Wiley and Sons, Inc., 1965, pp. 38-39.

TABLE I. - EXPERIMENTAL DATA

(a) U.S. Customary Units

Run	Data point	Liquid flow rate, W_l, lb/hr	Liquid inlet temperature, $T_{l,in}$, ^oF	Rotative acceleration, a/g, g's	Heat flux, Q/A, Btu/(hr)(ft^2)	Wall surface temperature, T_w, ^oF	Local fluid temperature, T_f, ^oF	Vapor exit pressure, $P_{v,e}$, in. Hg abs	Vapor exit saturation temperature, $T_{sat,v}$, ^oF	Vapor exit temperature, $T_{v,e}$, ^oF	Fluid annulus thickness, in.	Wall surface saturation temperature, $T_{sat,w}$, ^oF	Calorimeter		Vapor exit quality, percent or Vapor superheat, ^oF (as noted)	Heat transfer coefficient, h, Btu/(hr)(ft^2)(^oF)	Remarks
													Pressure, in. Hg abs	Temperature, ^oF			
Preliminary data																	
	1	-----	172	222	58 500	-----	-----	29.32	-----	215.5	-----	-----	-----	-----	[a]4 to 6 [a]5	----	NASA Lewis calorimeter
	2	-----	166	232	39 000	-----	-----	29.29	-----	216	-----	-----	-----	-----			
	3	-----	166	227	88 000	-----	-----	29.3	-----	214	-----	-----	-----	-----	[a]2 to 4	----	
	4	-----	148	68	117 000	-----	-----	29.20	-----	210.8	-----	-----	7.0	184.5	99.2	----	
	5	-----	161	142	117 000	-----	-----	29.18	-----	210.9	-----	-----	7.18	186.5	99.3	----	
	6	-----	171	143	175 000	-----	-----	29.22	-----	210.8	-----	-----	7.22	186	99.3	----	
	7	-----	173	143	175 000	-----	-----	29.20	-----	210.9	-----	-----	7.3	186.5	99.3	----	
	8	-----	171	230	117 000	-----	-----	29.20	-----	216 to 219	-----	-----	7.0	195	99.8	----	
	9	-----	171	235	117 000	-----	-----	29.20	-----	216	-----	-----	7.2	195	[a]5 to 8 99.8 [a]5	----	
	10	-----	172	82	117 000	-----	-----	29.16	-----	210.9	-----	-----	7.16	186.5	99.3	----	
	11	-----	192	81	234 000	-----	-----	28.95	-----	210.6	-----	-----	6.75	184.5		----	
	12	-----	190			-----	-----	28.97	-----	210.5	-----	-----	6.87	185		----	
	13	-----	203			-----	-----	28.96	-----	210.6	-----	-----	6.86	185		----	
	14	-----	208			-----	-----	28.95	-----	210.6	-----	-----	6.95	185.5		----	"
	15	-----	70	82	117 000	-----	-----	29.24	-----	211	-----	-----	21.2	200.3	99.7	----	Commercial calorimeter
	16	-----	71	230	117 000	-----	-----	29.19	-----	210	-----	-----	22.4	200	99.6	----	(used hereinafter)
	17	-----	104	21	25 400	-----	-----	29.13	-----	210.7	-----	-----	25.1	193	99.2	----	
	18	-----	113	21	60 500	-----	-----	29.13	-----	210.7	-----	-----	24.5	200	99.5	----	

Series A data

1	19	-----	138	15	14 900	233.2	207.3	29.04	210.5	210.5	8/16	211.3	-----	-----	----	682	
	20	-----	136	25	13 600	231.7	207.8				10/16	212.1	-----	-----	----	695	
	21	-----	129	50	13 400	229.9	207.5				10/16	213.7	-----	-----	----	827	
	22	-----	125	100	13 250	229.3	206.2				15/32	215.4	-----	-----	----	954	
	23	-----	128	200	12 960	232.9	203.9			210.6	7/16	219.6	-----	-----	----	973	Very little boiling
2	24	-----	144	15	30 200	240.2	208.4			210.5	8/16	211.3	24.0	200	99.5	1043	Vigorous boiling
	25	-----	147	25	30 600	240.1	207.9				9/16	211.9		201		1083	Vigorous boiling
	26	-----	147	50	30 400	238.8	205.5				7/16	212.9		201		1170	Moderate boiling
	27	-----	147	100	30 300	237.4	205.3				7/16	215.1		200		1360	Moderate boiling
	28	-----	144	200	30 000	239.4	204.6				13/32	218.9	24.5	200		1460	Very little boiling
3	29	-----	156	15	61 000	241.7	208.3				5/16	211.0	-----	-----	----	1990	Vigorous boiling
	30	-----	159	25	61 600	242.5	208.0				6/16	211.5	-----	-----	----	1990	Vigorous boiling
	31	-----	161	50	61 600	244.5	208.4				13/32	212.7	-----	-----	----	1940	Moderate boiling
	32	-----	163	100	61 400	245.2	206.9			210.6	7/16	215.3	-----	-----	----	2050	Moderate boiling
	33	-----	163	200	61 000	247.0	206.3			210.5	13/32	218.9	-----	-----	----	2170	Moderate boiling
4	34	[b]14.1	169	15	89 300	244.2	208.6	29.08	210.6	210.6	7/32	211.0	20.4	195	99.4	2690	Vigorous boiling
	35		171	25	89 500	245.1	208.5				4/16	211.3	20.4			2650	Vigorous boiling
	36		172	50	89 700	247.4	208.2				5/16	212.4	20.5			2560	Vigorous boiling
	37		172	100	88 800	249.0	207.8				6/16	214.7	20.5			2590	Moderate boiling
	38		172	200	88 000	251.0	207.4				6/16	218.5	20.5			2710	Moderate boiling
5	39	[b]20.8	175	15	117 500	246.0	209.4	29.10			5/32	210.9	-----	-----	----	3350	Vigorous boiling
	40		177	25		246.7	208.9			210.5	7/32	211.1	20.5	195	99.4	3300	
	41		177	50		249.0	208.1			210.5	5/16	212.3	-----	-----	----	3210	
	42		178	100		251.2	208.1			210.6	5/16	214.2	-----	-----	----	3170	
	43		178	200		253.9	207.6			210.6	11/32	218.0	-----	-----	----	3270	Moderate boiling

[a]Vapor superheat.
[b]Average for run.

TABLE I. - Continued. EXPERIMENTAL DATA

(a) Concluded. U.S. Customary Units

Run	Data point	Liquid flow rate, W_l, lb/hr	Liquid inlet temperature, $T_{l,in}$, ^oF	Rotative acceleration, a/g, g's	Heat flux, Q/A, Btu/(hr)(ft^2)	Wall surface temperature, T_w, ^oF	Local fluid temperature, T_f, ^oF	Vapor exit pressure, $P_{v,e}$, in. Hg abs	Vapor exit saturation temperature, $T_{sat,v}$, ^oF	Vapor exit temperature, $T_{v,e}$, ^oF	Fluid annulus thickness, in.	Wall surface saturation temperature, $T_{sat,w}$, ^oF	Calorimeter		Vapor exit quality, percent	Heat transfer coefficient, h, Btu/(hr)(ft^2)(^oF)	Remarks
													Pressure, in. Hg abs	Temperature, ^oF			
						Series A data											
6	44	[b]33.4	184	15	185 300	249.1	210.2	29.12	210.6	210.6	2/16	210.8	-----	-----	----	4840	Fluid level fluctuating
	45	↓	184	25	↓	250.1	209.1	↓	↓	↓	7/32	211.3	20.5	195	99.4	4780	Vigorous boiling
	46		185	50		251.5	208.7				9/32	212.2	20.6	↓	↓	4720	↓
	47		185	100		255.5	208.3				5/16	214.2	20.5			4490	
	48		185	200		259.1	208.3				11/32	218.0	20.4			4520	
7	49	[b]63.5	189	25	350 000	256.3	210.0	29.15	210.7		9/32	211.4	-----	-----	----	7800	
	50	↓	191	50	↓	258.7	209.3	↓	↓		11/32	212.6	-----	-----	----	7590	↓
	51		191	100		261.3	208.4			↓	6/16	214.7	-----	-----	----	7510	Moderate boiling
	52		191	200		265.8	208.3			210.7	23/64	218.5	20.15	194.5	99.5	7400	Moderate boiling
8	53	-----	164	25	27 800	236.0	208.2	29.10	210.6	210.6	10/16	212.2	-----	-----	----	1170	
	54	-----	164	↓	58 600	244.0	208.5	↓	↓	↓	8/16	212.0	-----	-----	----	1830	
	55	18.3	171		113 700	248.9	209.2				4/16	211.3	-----	-----	----	3020	
	56	30.0	180		171 000	251.3	210.3				10/16	212.2	-----	-----	----	4370	Bubbly froth
	57	22.0	180		129 000	249.2	208.5			↓	4/16	211.3	-----	-----	----	3410	
	58	-----	173		75 000	246.0	208.5			210.7	6/16	211.7	-----	-----	----	2190	
	59	-----	168	↓	38 200	240.3	208.3	↓	↓	210.7	7/16	211.9	-----	-----	----	1340	

Series B data

9	60	-----	141	200	12 400	233.1	199.3	29.05	210.5	210.5	15/32	220.0	-----	-----	----	950	Feeble boiling
	61	-----	146		27 600	239.6	199.6				15/32	220.0	-----	-----	----	1410	Feeble boiling
	62	-----	155		58 700	247.6	200.0				15/32	220.0	-----	-----	----	2130	Feeble boiling
	63	15.0	166		95 000	255.5	200.3				7/16	219.4	-----	-----	----	2630	
	64	30.6	181		167 000	263.9	200.8	29.06			7/16	219.4	-----	-----	----	3750	
	65	46.0	189		256 000	266.5	202.7	29.07			13/32	218.9	-----	-----	----	5380	Moderate boiling
	66	63.4	192		357 000	269.8	203.9	29.09	210.6		13/32	218.9	-----	-----	----	7020	Moderate boiling
	67	86.4	194		505 000	274.3	205.3	29.16	210.7	210.6	7/16	219.6	-----	-----	----	9220	Vigorous boiling
10	68	-----	166	50	16 370	230.9	207.2	29.05	210.5	210.4	10/16	213.6	-----	-----	----	945	Feeble boiling
	69	-----	161		33 300	239.5	209.4			210.4	8/16	213.1	-----	-----	----	1260	Feeble boiling
	70	-----	164		62 800	248.4	206.9			210.4	7/16	212.8	-----	-----	----	1760	
	71	15.6	171		99 000	254.9	208.3			210.5	7/16	212.9	-----	-----	----	2360	Moderate boiling
	72	30.0	181		169 000	258.8	208.5	29.06		210.5	6/16	212.6	-----	-----	----	3660	Moderate boiling
	73	45.1	188		236 000	260.8	208.7	29.07		210.5	6/16	212.6	-----	-----	----	4900	Vigorous boiling
	74	63.4	192		356 000	264.3	209.0	29.09	210.6	210.6	7/16	213.0	-----	-----	----	6930	
	75	82.6	194		468 000	267.0	211.8	29.16	210.7	210.6	15/32	213.1	-----	-----	----	8700	
11	76	-----	172	25	16 510	233.2	208.8	29.05	210.5	210.5	10/16	212.1	-----	-----	----	785	
	77	-----	166		34 700	239.8	206.4				9/16	212.0	-----	-----	----	1250	
	78	-----	167		61 200	247.8	211.0				8/16	211.8	-----	-----	----	1700	
	79	16.5	171		90 300	251.6	212.1				11/32	211.4	-----	-----	----	2250	
	80	30.9	183		173 500	257.7	213.2	29.06			5/16	211.3	-----	-----	----	3740	
	81	52.8	190		281 000	262.6	211.4	29.08	210.6		5/16	211.3	-----	-----	----	5480	
12	82	-----	170	15	16 100	233.5	208.5	29.05	210.5		10/16	211.5	-----	-----	----	735	
	83	-----	166		33 700	239.7	210.0				10/16	211.5	-----	-----	----	1200	
	84	-----	165		66 000	245.0	211.8				7/16	211.2	-----	-----	----	1950	
	85	15.1	170		100 000	251.7	212.0				7/32	210.9	-----	-----	----	2450	
	86	33.5	181		179 500	256.4	211.0	29.06			3/16	210.8	-----	-----	----	3920	
13	87	-----	---	[c]0	16 400	230.0	208.2	29.05		210.6	-----	210.6	-----	-----	----	850	Nonrotating
	88	-----	166		36 300	236.8	207.7				-----		-----	-----	----	1380	
	89	-----	168		64 500	241.6	208.3				-----		-----	-----	----	2080	
	90	-----	178		101 000	245.7	208.4				-----		-----	-----	----	2870	
	91	-----	187		147 000	250.3	208.7				-----		-----	-----	----	3700	
	92	-----	191		188 000	253.7	209.1	29.06			-----		-----	-----	----	4360	
	93	-----	192		234 000	256.7	209.0	29.06			-----		-----	-----	----	5080	

[b]Average for run.

[c]Nonrotating, normal earth gravity.

TABLE I. - Continued. EXPERIMENTAL DATA

(b) SI Units

Run	Data point	Liquid flow rate, W_l, kg/hr	Liquid inlet temperature, $T_{l,in}$, ^oK	Rotative acceleration, a/g, g's	Heat flux, Q/A, kW/m^2	Wall surface temperature, T_w, ^oK	Local fluid temperature, T_f, ^oK	Vapor exit pressure, $P_{v,e}$, $\frac{kN}{m^2}$ abs	Vapor exit saturation temperature, $T_{sat,v}$, ^oK	Vapor exit temperature, $T_{v,e}$, ^oK	Fluid annulus thickness, cm	Wall surface saturation temperature, $T_{sat,w}$, ^oK	Calorimeter		Vapor exit quality, percent or Vapor superheat, ^oK (as noted)	Heat transfer coefficient, h, $kW/(m^2)(^oK)$	Remarks
													Pressure, $\frac{kN}{m^2}$ abs	Temperature, ^oK			
								Preliminary data									
	1	-----	351	222	185	-----	-----	99.10	-----	375.1	----	-----	-----	-----	[a]2 to 3	-----	NASA Lewis calorimeter
	2	-----	348	232	123	-----	-----	99.00	-----	375.4	----	-----	-----	-----	[a]3	-----	↓
	3	-----	348	227	278	-----	-----	99.03	-----	374.5	----	-----	-----	-----	[a]1 to 2	-----	↓
	4	-----	338	68	369	-----	-----	98.70	-----	372.5	----	-----	23.66	358	99.2	-----	↓
	5	-----	345	142	369	-----	-----	98.63	-----	↓	----	-----	24.27	359	99.3	-----	↓
	6	-----	351	143	552	-----	-----	98.76	-----	↓	----	-----	24.40	359	99.3	-----	↓
	7	-----	352	143	552	-----	-----	98.70	-----	↓	----	-----	24.67	359	99.3	-----	↓
	8	-----	351	230	369	-----	-----	98.70	-----	375 to 377	----	-----	23.66	364	99.8	-----	↓
	9	-----	351	235	369	-----	-----	98.70	-----	375.4	----	-----	24.34	364	[a]3 to 4 99.8 [a]3	-----	↓
	10	-----	352	82	369	-----	-----	98.56	-----	372.5	----	-----	24.20	359	99.3	-----	↓
	11	-----	362	81	738	-----	-----	97.85	-----	372.4	----	-----	22.82	358	↓	-----	↓
	12	-----	361	↓	↓	-----	-----	97.92	-----	↓	----	-----	23.22	358	↓	-----	↓
	13	-----	368	↓	↓	-----	-----	97.88	-----	↓	----	-----	23.19	358	↓	-----	↓
	14	-----	371	↓	↓	-----	-----	97.85	-----	↓	----	-----	23.49	358	↓	-----	Commercial calorimeter
	15	-----	294	82	369	-----	-----	98.83	-----	372.5	----	-----	71.66	366.7	99.7	-----	(used hereinafter)
	16	-----	295	230	369	-----	-----	98.66	-----	372.0	----	-----	75.71	366.5	99.6	-----	↓
	17	-----	313	21	80	-----	-----	98.46	-----	372.5	----	-----	84.84	363	99.2	-----	↓
	18	-----	318	21	191	-----	-----	98.46	-----	372.5	----	-----	82.81	366.5	99.5	-----	↓

Series A data

1	19	-----	332	15	47	384.9	370.5	98.16	372.3	372.3	1.3	372.8	-----	-----	----	3.88	
	20	-----	331	25	42.9	384.1	370.8			↓	1.6	373.2	-----	-----	----	3.95	
	21	-----	327	50	42.2	383.1	370.6				1.6	374.1	-----	-----	----	4.70	
	22	-----	325	100	41.8	382.8	369.9				1.2	375.0	-----	-----	----	5.41	
	23	-----	327	200	40.9	384.8	368.6			372.4	1.1	377.4	-----	-----	----	5.52	Very little boiling
2	24	-----	336	15	95.3	388.8	371.1			372.3	1.3	372.8	81.12	367	99.5	5.93	Vigorous boiling
	25	-----	337	25	96.5	388.8	370.9				1.4	373.1	↓	367	↓	6.15	*Vigorous boiling*
	26	-----	337	50	95.9	388.0	369.5				1.1	373.6		367		6.64	Moderate boiling
	27	-----	337	100	95.6	387.3	369.4				1.1	374.9	↓	367		7.73	Moderate boiling
	28	-----	336	200	94.6	388.4	369.0				1.0	377.0	82.81	367	↓	8.29	Very little boiling
3	29	-----	342	15	192	389.6	371.1				.8	372.6	-----	-----	-----	11.3	Vigorous boiling
	30	-----	344	25	194	390.1	370.9				.95	372.9	-----	-----	-----	11.3	Vigorous boiling
	31	-----	345	50	194	391.2	371.1	↓	↓	↓	1.0	373.5	-----	-----	-----	11.0	Moderate boiling
	32	-----	346	100	193	391.6	370.3			372.4	1.1	375.0	-----	-----	-----	11.6	Moderate boiling
	33	-----	346	200	192	392.6	370.0			372.3	1.0	377.0	-----	-----	-----	12.3	Moderate boiling
4	34	[b]6.4	349	15	282	391.0	371.3	98.29	372.4	372.4	.55	372.6	68.95	364	99.4	15.3	Vigorous boiling
	35	↓	351	25	282	391.5	371.2				.65	372.8	68.95	↓	↓	15.0	Vigorous boiling
	36		351	50	283	392.8	371.0	↓	↓	↓	.8	373.4	69.29			14.5	Vigorous boiling
	37		351	100	280	393.7	370.8				.95	374.6	69.29			14.7	Moderate boiling
	38	↓	351	200	278	394.8	370.6				.95	376.8	69.29	↓	↓	15.4	Moderate boiling
5	39	[b]9.4	353	15	371	392.0	371.7	98.36		↓	0.4	372.5	-----	-----	-----	18.9	Vigorous boiling
	40		354	25		392.4	371.4		↓	372.3	.55	372.6	69.29	364	99.4	18.7	↓
	41		354	50	↓	393.7	371.0	↓		372.3	.8	373.3	-----	-----	-----	18.2	
	42		354	100		394.9	371.0		↓	372.4	.8	374.4	-----	-----	-----	18.0	↓
	43	↓	354	200	↓	396.4	370.7	↓		372.4	.9	376.5	-----	-----	-----	18.6	Moderate boiling

[a]Vapor superheat.
[b]Average for run.

TABLE I. - Concluded. EXPERIMENTAL DATA

(b) Concluded. SI Units

Run	Data point	Liquid flow rate, W_l, kg/hr	Liquid inlet temperature, $T_{l,in}$, ^oK	Rotative acceleration, a/g, g's	Heat flux, Q/A, kW/m^2	Wall surface temperature, T_w, ^oK	Local fluid temperature, T_f, ^oK	Vapor exit pressure, $P_{v,e}$, $\frac{kN}{m^2}$ abs	Vapor exit saturation temperature, $T_{sat,v}$, ^oK	Vapor exit temperature, $T_{v,e}$, ^oK	Fluid annulus thickness, cm	Wall surface saturation temperature, $T_{sat,w}$, ^oK	Calorimeter		Vapor exit quality, percent	Heat transfer coefficient, h, $kW/(m^2)(^oK)$	Remarks
													Pressure, $\frac{kN}{m^2}$ abs	Temperature, ^oK			
							Series A data										
6	44	[b]15.1	358	15	585	393.8	372.1	98.43	372.4	372.4	0.3	372.5	-----	---	----	27.5	Fluid level fluctuating
	45			25		394.3	371.5				.55	372.8	69.29	364	99.4	27.1	Vigorous boiling
	46			50		395.1	371.3				.7	373.3	69.63			26.8	
	47			100		397.3	371.1				.8	374.4	69.29			25.5	
	48			200		399.3	371.1				.9	376.5	68.95			25.7	
7	49	[b]28.8	361	25	1104	397.8	372.0	98.53			.7	372.8	-----	---	----	44.3	
	50		362	50		399.1	371.6				.9	373.5	-----	---	----	43.1	
	51		362	100		400.5	371.1				.95	374.6	-----	---	----	42.7	Moderate boiling
	52		362	200		403.0	371.1				.9	376.8	68.11	363	99.5	42.0	Moderate boiling
8	53	-----	347	25	87.7	386.5	371.0	98.36			1.6	373.3	-----	---	----	6.64	
	54	-----	347		185	390.9	371.2				1.3	373.1	-----	---	----	10.4	
	55	8.3	351		359	393.6	371.6				.65	372.8	-----	---	----	17.2	
	56	13.6	356		540	395.0	372.2				1.6	373.3	-----	---	----	24.8	Bubbly froth
	57	10.0	356		407	393.8	371.2				.65	372.8	-----	---	----	19.4	
	58	-----	352		237	392.0	371.2				.95	373.0	-----	---	----	12.4	
	59	-----	349		120	388.9	371.1				1.1	373.1	-----	---	----	7.6	

Series B data

9	60	-----	334	200	39.2	384.9	366.1	98.19	372.3	372.3	1.2	377.6	-----	---	----	5.4	Feeble boiling
	61	-----	337		87	388.5	366.3				1.2	377.6	-----	---	----	8.0	Feeble boiling
	62	-----	342		185	392.9	366.5				1.2	377.6	-----	---	----	12.1	Feeble boiling
	63	6.8	348		300	397.3	366.6				1.1	377.3	-----	---	----	14.9	
	64	13.9	356		527	402.0	366.9	98.22			1.1	377.3	-----	---	----	21.3	
	65	20.9	361		807	403.4	368.0	98.26			1.0	377.0	-----	---	----	30.5	Moderate boiling
	66	28.8	362		1125	405.3	368.6	98.32	372.4		1.0	377.0	-----	---	----	39.8	Moderate boiling
	67	39.2	363		1590	407.8	369.4	98.56	372.4	372.4	1.1	377.4	-----	---	----	52.3	Vigorous boiling
10	68	-----	348	50	51.6	383.6	370.5	98.19	372.3	372.3	1.6	374.0	-----	---	----	5.36	Feeble boiling
	69	-----	345		105	388.4	371.7				1.3	373.8	-----	---	----	7.15	Feeble boiling
	70	-----	347		198	393.4	370.3				1.1	373.6	-----	---	----	10.0	
	71	7.1	351		312	397.0	371.1				1.1	373.6	-----	---	----	13.4	Moderate boiling
	72	13.6	356		533	399.1	371.2	98.22			.95	373.5	-----	---	----	20.8	Moderate boiling
	73	20.5	360		745	400.3	371.3	98.26			.95	373.5	-----	---	----	27.8	Vigorous boiling
	74	28.8	362		1122	402.2	371.5	98.32	372.4	372.4	1.1	373.7	-----	---	----	39.4	
	75	37.5	363		1477	403.7	373.0	98.56	372.4	372.4	1.2	373.8	-----	---	----	49.5	
11	76	-----	351	25	52.1	384.9	371.4	98.19	372.3	372.3	1.6	373.2	-----	---	----	4.46	
	77	-----	348		109.4	388.6	370.0				1.4	373.1	-----	---	----	7.10	
	78	-----	348		193	393.0	372.6				1.3	373.0	-----	---	----	9.65	
	79	7.5	351		285	395.1	373.2				.9	372.8	-----	---	----	12.8	
	80	13.9	357		547	398.5	373.8	98.22			.8	372.8	-----	---	----	21.2	
	81	23.9	361		886	401.3	372.8	98.29	372.4		.8	372.8	-----	---	----	31.1	
12	82	-----	350	15	50.8	385.1	371.2	98.19	372.3		1.6	372.9	-----	---	----	4.17	
	83	-----	348		106.2	388.5	372.0				1.6	372.9	-----	---	----	6.81	
	84	-----	347		208	391.5	373.0				1.1	372.7	-----	---	----	11.1	
	85	6.9	350		315	395.2	373.1				.55	372.5	-----	---	----	13.9	
	86	15.2	356		566	397.8	372.6	98.22			.5	372.5	-----	---	----	22.2	
13	87	-----	---	[c]0	51.8	383.1	371.0	98.19		372.4	----	372.4	-----	---	----	4.83	Nonrotating
	88	-----	348		114.4	386.9	370.8				----		-----	---	----	7.84	
	89	-----	349		204	389.6	371.1				----		-----	---	----	11.8	
	90	-----	354		318	391.9	371.1				----		-----	---	----	16.3	
	91	-----	359		464	394.4	371.3				----		-----	---	----	21.0	
	92	-----	362		594	396.3	371.5	98.22			----		-----	---	----	24.8	
	93	-----	362		738	398.0	371.5	98.22			----		-----	---	----	28.9	

[b]Average for run.

[c]Nonrotating, normal earth gravity.

Motion-picture film supplement C-253 is available on loan. Requests will be filled in the order received. You will be notified of the approximate date scheduled.

The film (16 mm, 14 min, color, sound) presents high-speed motion pictures of boiling activity and behavior of the interface between liquid and vapor in the rotating boiler at accelerations from 25 to 400 g's. It illustrates the effects of heat flux and rotative acceleration on the bubble population, size, and motion. With stop-action and animation, several interesting boiling features are revealed, such as the convective secondary-flow cells at high g's, the bursting of vapor domes at the interface, and the motion of liquid droplets and jets in the vapor space. The suppression of boiling and quieting of the interface caused by increasing the acceleration is graphically shown, as well as the opposite effects caused by increasing the heat input from 0.9 to 24 kilowatts.

Requests for the film should be addressed to:

Chief, Technical Information Division (5-5)
NASA Lewis Research Center
21000 Brookpark Road
Cleveland, Ohio 44135

CUT

Date _____

Please send, on loan, copy of film supplement C-253 to
TN D-4136

_____
Name of Organization

_____
Street Number

_____
City and State Zip Code

Attention: Mr. _____
Title _____

"The aeronautical and space activities of the United States shall be conducted so as to contribute . . . to the expansion of human knowledge of phenomena in the atmosphere and space. The Administration shall provide for the widest practicable and appropriate dissemination of information concerning its activities and the results thereof."

—NATIONAL AERONAUTICS AND SPACE ACT OF 1958

NASA SCIENTIFIC AND TECHNICAL PUBLICATIONS

TECHNICAL REPORTS: Scientific and technical information considered important, complete, and a lasting contribution to existing knowledge.

TECHNICAL NOTES: Information less broad in scope but nevertheless of importance as a contribution to existing knowledge.

TECHNICAL MEMORANDUMS: Information receiving limited distribution because of preliminary data, security classification, or other reasons.

CONTRACTOR REPORTS: Scientific and technical information generated under a NASA contract or grant and considered an important contribution to existing knowledge.

TECHNICAL TRANSLATIONS: Information published in a foreign language considered to merit NASA distribution in English.

SPECIAL PUBLICATIONS: Information derived from or of value to NASA activities. Publications include conference proceedings, monographs, data compilations, handbooks, sourcebooks, and special bibliographies.

TECHNOLOGY UTILIZATION PUBLICATIONS: Information on technology used by NASA that may be of particular interest in commercial and other non-aerospace applications. Publications include Tech Briefs, Technology Utilization Reports and Notes, and Technology Surveys.

Details on the availability of these publications may be obtained from:

SCIENTIFIC AND TECHNICAL INFORMATION DIVISION

NATIONAL AERONAUTICS AND SPACE ADMINISTRATION

Washington, D.C. 20546